CONFIDENTIAL

NATIONAL AERONAUTICS AND SPACE ADMINISTRATION
CONTRACT NO. NASw-6

GROUP 4
Downgraded at 3 year intervals; declassified after 12 years

Quarterly Summary Report No. 38-1

Nondestructive Solid Propellant Testing

Copy No._____

JET PROPULSION LABORATORY
CALIFORNIA INSTITUTE OF TECHNOLOGY
PASADENA, CALIFORNIA

August 31, 1960

CONFIDENTIAL

Preface

This Quarterly Summary Report chronicles the progress of research in the area of the nondestructive testing of solid-propellant rocket motors, carried out at the Jet Propulsion Laboratory.

Section I of the Report serves as a summary and survey of the problems to which the testing program is addressed; Section II details results and progress in specific areas of research; Section III presents a continuing search of the technical literature of this field, organized under four method areas.

The work reported herein is undertaken in partial fulfillment of Advanced Research Projects Agency Letter Order No. 107-60, for the National Aeronautics and Space Administration.

This initial issue of the Report covers the period from the inception of the project up to August 31, 1960.

W. H. Pickering, *Director*
Jet Propulsion Laboratory

This document contains information affecting the national defense of the United States, within the meaning of the Espionage Laws, Title 18, U.S.C., Sections 793 and 794, the transmission or revelation of which in any manner to an unauthorized person is prohibited by law.

Copyright © 1960
Jet Propulsion Laboratory
California Institute of Technology

Contents

I. Introduction 1
A. Major Types of Defects 2
B. Summary 4

II. Physical Properties Studies 6
A. Effects of Moisture on Mechanical Properties 6
B. Volume Changes Under Tensile Deformations 15
C. Motor Strain Testing 18

III. Bibliography 27
A. Radiography 27
B. Ultrasonics 32
C. Infrared 34
D. Miscellaneous 34

References 38

I. INTRODUCTION

This project has as an objective the determination of generalized techniques for detecting the abnormalities in solid propellant grains which cause malfunction of the rocket, and for predicting the degree of malfunction which the abnormality will cause.

Tenney (Ref 1) cites the "importance of nondestructive testing in detecting the following three possible defects: (1) bubbles and voids, (2) cracks in more or less radial direction, (3) lack of bonding between grain and liner and liner and casing." In a later paper (Ref 2), he adds to the list of defects two other factors: (1) the influence of aging and (2) the influence of handling during shipment.

Certain recognized techniques are available for the detection of these defects, and they are discussed in considerable detail in a number of papers in the Bibliography. The most generally used test methods can be summarized briefly:

(1) X-ray radiography.

(2) Isotope gammagraphy with a cobalt-60 source.

(3) Fluoroscopy and fluorography.

(4) Gamma scintillation.

(5) Visual inspection: naked eye and borescope.

(6) Ultrasonics.

(7) Infrared.

The sensitivity of these techniques and their applicability to the detection of specific abnormalities are also covered thoroughly in the literature.

Blatz (Ref 3) states, "... the question of measurement of defects implies the ability to predict motor failure." A further implication of testing theory would then demand that there be known acceptance criteria under which the presence of certain defects can be tolerated. It is customary in the solid-propellant industry to base the creation of acceptance or rejection criteria upon the experience of the motor manufacturer. This experience is generally the distillation of data from a large number of motors fabricated and fired. When it is known from inspection and subsequent firing that the presence of a known anomaly will not adversely affect the performance of a motor, this type of defect is classified acceptable. When an anomaly whose influence on performance is unknown from experience is detected, the motor will be static fired and the results evaluated. If an unsatisfactory performance can be attributed directly to the presence of this anomaly, it will be classified as cause for rejection. On this basis, certain generalized rules have come into use as guidelines governing the acceptability of motors. Insofar as the trend is toward engineering conservatism, very few motors are accepted which later prove to be unsatisfactory.

A. Major Types of Defects

1. Voids or Bubbles

The two principal causes for the formation of voids or bubbles in composite grains are:

(1) Inclusion of air during casting.

(2) Chemical reaction other than polymerization, after casting and during cure, with the evolution of gaseous reaction products. A manifestation of this is grain porosity.

A void or porous section in the web can adversely affect the performance of the motor in one or more of several ways. It can cause a part of the burning surface to reach the case wall before the bulk of the grain has been consumed. The length of time that the unprotected case wall will thus be exposed to the flame temperature is a function of the radial depth of the void. Failure criteria can be established provided certain parameters are known. The most important of these parameters are the rate of temperature rise in the case wall at the hot spot and the deterioration of the material working strength as a function of temperature and of the abnormal stress distribution at the hot-spot boundary due to the temperature gradient. Knowledge of the thermal diffusivity and the dimensions of the wall material are also important. Finally the over-all heat-transfer coefficient from the combustion reaction products to the case must be known. This will be a function of the local gas velocity and the thermal resistance of the liner and any other insulation which is present.

It can be demonstrated that a void is more of a serious problem if it is located in or near a star-point trough than if it is located within the star point. Because of the higher rates of heat transfer near the aft end of the motor than near the head end due to the increased gas velocity, it would be expected that a void at the aft end would be more critical than one further forward. A porous section, because of the apparent increase in burning rate, could be expected to behave as a large void whose effective dimensions depend upon the extent of porosity. In high modulus grains, excessive porosity could create a condition of gas channeling which would lead to a failure of the grain and subsequent destruction of the motor.

The question of proximity of voids and the interrelationship of contiguous voids can be treated analytically. In an internal-burning grain, certain physical relationships obtain, and some reasonable assumptions can be made. Taking the simplest case of a spherical void, the succeeding events can be predicted if it is assumed that (1) burning propagates normal to all exposed surfaces, and (2) the entire void surface is ignited when the flame front passes the point of tangency between the void and the burning cylindrical surface. It can be established that as burning progresses the center of propagation of the void burning surface remains fixed (Fig 1). In the longitudinal planes the intersections of the spherical void burning surface and the cylindrical burning surface describe a series of parabolas. In the radial planes, the surface intersections describe a series of hyperbolas. The envelope of surfaces thus described traces the history of the new surface exposed by the void as propellant combustion progresses.

It is apparent that the distance between the unvoided surface of the propellant and the case wall at the time the void surface reaches the wall is equal to the diameter of the original void. A continuously increasing area of the case wall will then be exposed to the flame temperature for the time it takes to burn the remainder of the propellant in the chamber.

The conclusion derived from this line of reasoning is that the effect of the presence of a single void is independent of its radial position. Expressed in another way, a void which is near the wall of the motor will burn through to the wall in the same time as would a void of the same diameter which was originally nearer the center of the grain.

If two voids are placed such that the line of centers passes through and is perpendicular to the longitudinal axis of the grain, then the burning surface will reach the case wall while the unburned web has a thickness equal to the sum of the diameters of the voids. If two voids are placed such that one falls within the envelope of surfaces generated by the void nearer the center of the grain, then the web thickness at the time of burnthrough to the wall will be a function of the diameters of the voids and their position with respect to each other. If two voids are present, one of which does not lie within the envelope of surfaces generated by the other, then the effects of their presence are completely independent, and the void with the larger diameter will propagate to the wall first.

Up to this point, the effect of the physical parameters of the grain has not been considered. This subject is far too complex to be analyzed superficially. A program to study the behavior of a propellant grain is discussed in more detail in a later section of this report. It will suffice here to make one general observation. When an internal-burning case-bonded grain in a thin-walled chamber is pressurized on ignition, the pressure force will cause both the grain and the case wall to expand. The compressive radial strain will vary in magnitude throughout the web, being greatest at the inner periphery and least at the case wall. In this discussion it will not be necessary to deter-

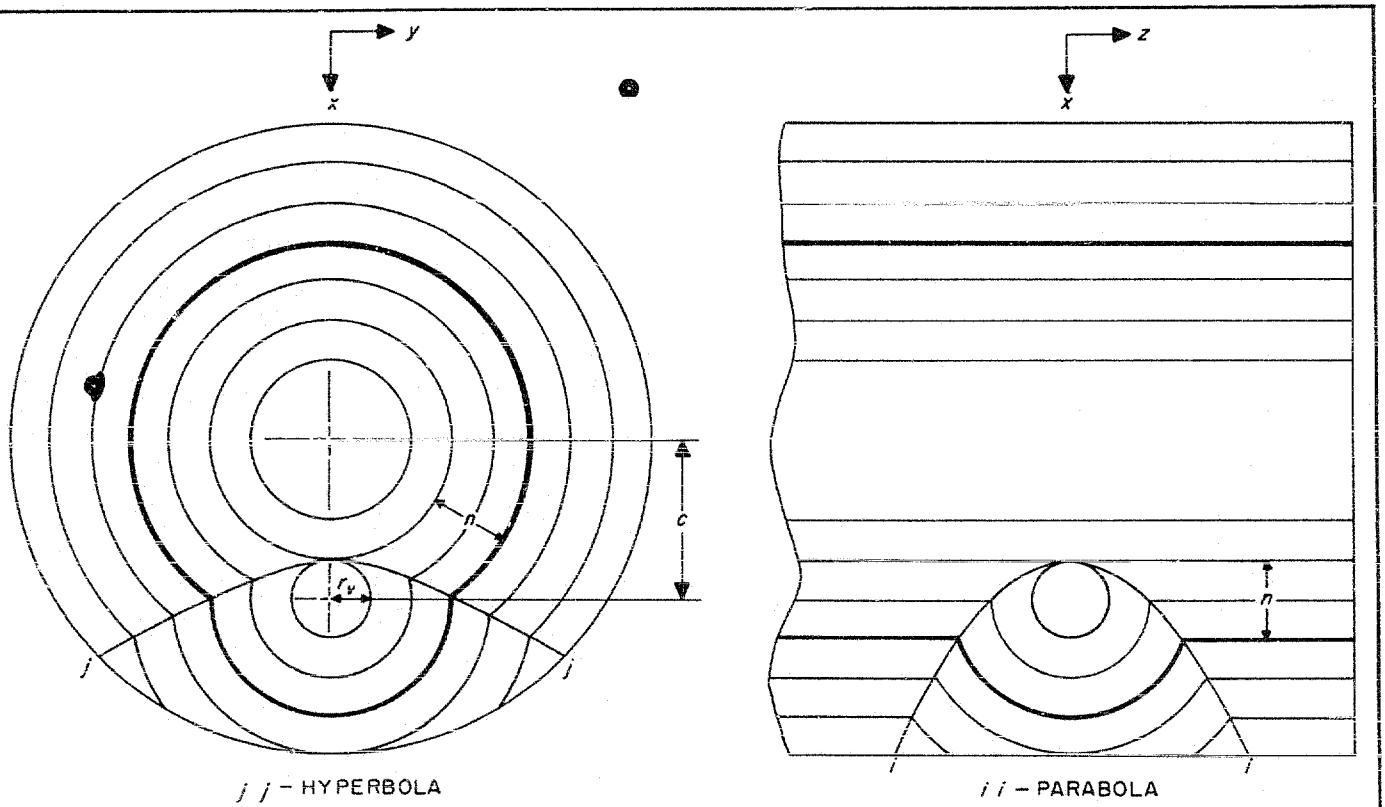

$$\frac{\left(x-\frac{c}{2}\right)^2}{\left(\frac{c}{2}-r_v\right)^2}-\frac{y^2}{2r_v(c-r_v)}=1$$

$$z^2=2r_v(2r_v-2c+2x)$$

$$A_B=2\pi(c-r_v+n)l+4\int_E^{c+r_v}\int_0^F r_v\left[(c-r_v+n)^2-x^2\right]^{-\frac{1}{2}}dx\,dz-4\int_E^{c-r_v+n}\int_0^F(c-r_v+n)\left[r_v^2-(x-c)^2-z^2\right]^{-\frac{1}{2}}dx\,dz$$

where A_B is burning-surface area, $E=c+\frac{n^2}{2c}+n-r_v-\frac{nr_v}{c}$, and $F=[2c(x-E)]^{\frac{1}{2}}$

Figure 1. Burning-surface model with vacuole, internal-burning grain

mine the actual strain distribution, except to note that it is non-linear. The peripheral surface of a void near the center of the grain will be in a greater state of strain than that of a similar void near the case wall. Consequently, the possibility of initiating grain rupture being greatest where the strain is greatest, a void near the center of the grain would have a more deleterious effect than one near the case wall.

Attention has been directed to the increase in chamber pressure to be expected when a burnthrough to a void occurs and additional surface is exposed to combustion. The possibility of the increased pressure exceeding the design specifications of the case material has been considered. Two examples can be cited to evaluate the probability of such an occurrence.

Consider an end-burning charge containing within it a spherical void. Combustion will be initiated on the exposed surface, and it will be assumed that all points on the surface are simultaneously ignited and that burning is propagated normal to this surface. Insofar as the burning-surface area remains constant, the chamber pressure will remain constant. As the burning surface recedes to the point of tangency with the void, it can be assumed that at burnthrough all the inner surface of the void is

simultaneously ignited. At this point, a step-function increase in pressure, reflecting the increased burning-surface area, would be anticipated. It can be easily demonstrated by the use of simple geometry or elementary calculus that as burning proceeds, and before any part of the burning surface reaches the case wall, there is no further increase in burning-surface area (Fig 2). In short, the total surface exposed to combustion after burnthrough is always equal to the sum of the original burning surface and the surface area of the void.

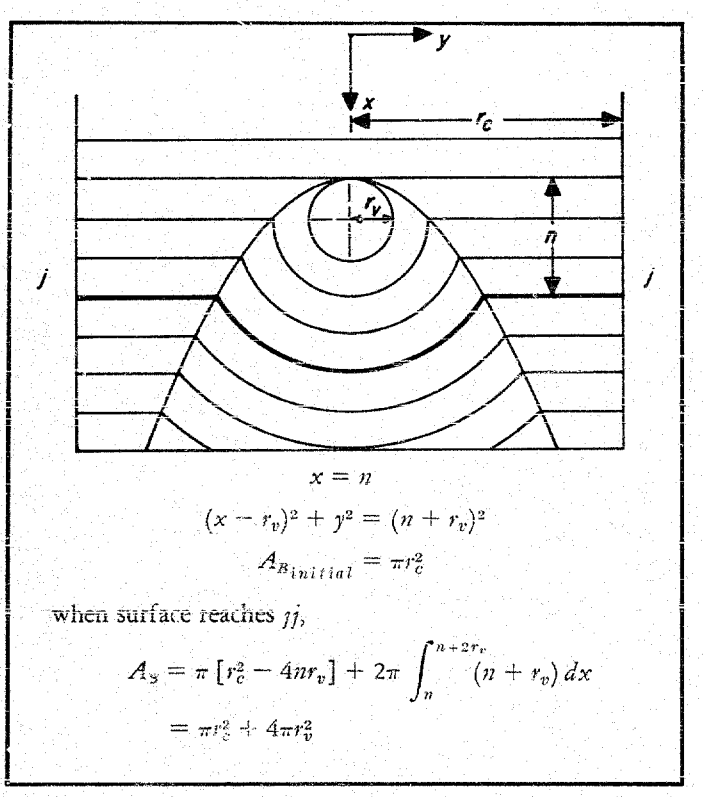

Figure 2. Burning-surface model with vacuole, end-burning grain

The analysis of the change in burning-surface area caused by the presence of a void in the web of an internal-burning grain is not quite so simple. Simple geometry is no longer an adequate tool, and the analytical expression is not easily integrated. If (Fig 1) the distance between the center of the void and the longitudinal axis of the grain c is very much larger than the radius of the void

$$c >> r_v$$

then the physical model will approach that shown in Figure 2. There is reasonable justification for the conclusion that the additional area of burning exposed by the void is approximately constant as burning proceeds, and is approximately equal to the original surface of the void.

2. Cracks

The presence of longitudinal cracks extending radially through the grain is, without further qualification, justifiable cause for rejection of the motor. The main problems associated with cracks are their detection and a determination of the means of preventing them.

Allegretto and Painter (Ref 4) have indicated that *flame propagation in a crack increases with increasing crack width and apparently reaches a plateau.* Their studies involved cracks from 0.0015 to 0.015 inch in width. Flame propagation down the sides of the crack was observed in all cases.

It is apparent that pressurization of the motor on ignition will strain the inner periphery of the grain, tending to widen any cracks already present. Consequently, a rupture of any measurable width at the inner periphery would be considered unsatisfactory.

It should be noted that inspection procedures for the detection of cracks or grain separation of any kind should be carried out at temperatures near the lower operating limit of the motor. The increased thermal loading, beyond normal ambient temperatures, will serve to increase the width of any cracks already present and facilitate their detection.

3. Lack of Bonding

Lack of bonding between propellant and liner or liner and case when it occurs in the domed ends, or in an area that can propagate into the domed ends, is generally considered to be cause for motor rejection. However, where the separation extends to the inner periphery and is observable, provision is sometimes included in motor-acceptance specifications for effecting repairs.

B. Summary

Ideally, in a discussion of nondestructive testing, all known modes of failure should be considered. One characteristic of most solid-propellant systems is the inability of the grain to withstand aging. Test procedures have

been devised to determine the extent to which aging instability is manifested, and a great deal of effort is being expended to investigate the basic parameters associated with these phenomena.

The conclusion is inescapable that a determination of the presence of anomalies by nondestructive techniques and an evaluation of their effect on motor behavior is not a complete approach to an understanding of solid-propellant grain phenomena. As was pointed out in the case of a cracked grain or certain unbonded grains, the presence of the defect requires no further evaluation. It insures the rejection of the motor.

Continuing inspection procedures are needed to monitor the condition of the motor from casting to firing. The first inspection should be designed to detect the presence of anomalies resulting from the processing of the grain including the initial thermal cycling from cure to ambient temperatures. Secondary inspection should be used to monitor the chemical and physical integrity of the grain during aging. Preferably a continuing technique such as an evaluation of the sonic or electric properties of the grain should be developed for this purpose.

One technique successfully used on the *Sergeant* motor is the determination of shore hardness during aging. The deterioration of hardness properties was correlated with the onset of slumping, and grains which would otherwise have been lost were saved for static test.

Basic failure criteria are needed to predict, from a knowledge of the propellant physical and chemical properties, from the grain and motor configuration, and from the anticipated operational environment, the ability of the grain to withstand cracking, or lack of bonding, or any other anomalous condition.

When the influence of specific parameters upon grain behavior is known, it will be possible to design motors where the probability of anomalous behavior is slight.

The investigation of the influence of propellant chemical parameters upon mechanical properties, and of mechanical properties upon grain behavior will constitute the major objective of this project.

II. PHYSICAL PROPERTIES STUDIES

A. Effects of Moisture on Mechanical Properties

Tensile properties of composite solid propellants are an important parameter used frequently in research and development work, process control, and surveillance studies. The temperature and strain rate during a tensile test have long been recognized as having a major effect on the results which are obtained, but the relative humidity is rarely reported. The recommended method of tensile testing (Ref 5) suggests that specimens be tested on the same day as prepared, and that ammonium perchlorate propellants be conditioned at 77°F and 50% relative humidity prior to test. However, these recommendations are seldom followed. Similarly, investigators at this Laboratory (Ref 6) and elsewhere have studied the storage stability of propellants at various temperatures, but during most of this work, little direct attention was given to the effect of moisture on the rate and extent of the observed changes in tensile properties.

A notable exception is the work carried out at Stanford Research Institute (Refs 7 to 11), which showed a pronounced difference in the shear strength of polysulfide propellants stored at low and high humidities. More recently, Davis (Ref 12) reported tensile data on several ammonium perchlorate propellants stored at different temperatures and humidities and found that their physical properties are greatly affected by both environmental conditions, and also that polyurethane propellants are more sensitive to the effects of high humidity than polysulfide systems.

1. Experimental Program

To expand on this work, a series of studies was made on the effects of humidity on the extent, rate, and reversibility of the changes in physical properties. The results of such studies should give information not only on the ultimate effects produced but also on the mechanism of moisture penetration into propellants. This section is concerned with the tensile properties of three polysulfide

and four polyurethane propellants containing ammonium perchlorate, after storage at ambient temperature and at several relative humidities.

a. Polysulfide propellant compositions. Three well-established polysulfide propellants were used in this work—their composition is given in Table 1. Propellants JPL 128 and JPL 136 both employ ethyl formal polysulfide LP-33 as the binder, and contain about 70% ammonium perchlorate; they differ principally in the curing system employed. It will be noted that neither of these propellants was cured sufficiently long at 160°F to develop optimum mechanical properties. JPL 138 uses a butyl formal polysulfide liquid polymer LP-205, and contains 80% ammonium perchlorate. Though this propellant was cured under optimum conditions of time and temperature, as indicated by existing plots of physical properties vs cure time, its initial elongation at maximum stress was much lower than normal (Ref 13). The reason for this discrepancy may become apparent when the effects of moisture are discussed.

b. Polyurethane propellant compositions. The polyurethane propellants all contained 80% ammonium perchlorate as a 70:30 bimodal blend and are described in Table 2. JPL X-500-1 is a basic formulation with a binder containing 0.10 mole of TMP per mole of PPG and sufficient TDI to give an NCO/OH ratio of 1.05 (Ref 14). Propellants X-532 and X-535 have physical properties superior to those of X-500-1, achieved by the addition of a commercial wetting agent, Alrosperse 11p. The X-532 binder contains 0.25 mole TMP per mole PPG, and Alrosperse is considered to be an inert ingredient (Ref 14). In X-535, on the other hand, the stoichiometry of the binder is adjusted for the known reactivity of Alrosperse, and the TMP content is reduced to 0.075 mole, resulting in a propellant with much greater elongation (Ref 15). The X-600 propellant is a formulation of a recently developed propellant family (Ref 16), in which urea groups are incorporated in the binder. The initial mechanical properties listed in Table 2 are typical for the cure conditions employed, although additional studies on cure conditions have since shown the sample to be undercured.

c. Experimental conditions. The propellants were mixed in a sigma-blade or planetary-type mixer, cast into 5 × 6-inch cylindrical molds, and cured in conformance with established procedures. Immediately after cure, the

Table 1. Composition and initial properties of polysulfide propellants[a]

Composition, wt %	JPL 128 C-199	JPL 136 C-198	JPL 138 C-197
Ammonium perchlorate, unground	49.7	50.52	68.00
Ammonium perchlorate, ground	21.3	21.45	12.00
LP-33 polysulfide liquid polymer	25.5	25.67	—
LP-205 polysulfide liquid polymer	—	—	17.64
p-Quinone dioxime	1.7	1.71	1.71
Diphenyl guanidine	0.8	—	—
Sulfur	—	0.15	0.15
Ferric oxide	1.0	—	—
Monastral blue	—	0.50	0.50
Cure conditions			
Cure temperature, °F	160	160	180
Cure time, hours	120	120	120
Initial mechanical properties			
Measured at 77°F			
Tensile strength, psi	60.0	84.9	215.7
Elongation at max stress, %	7.0	10.3	9.0
Typical, reported at 80°F[d]			
Tensile strength, psi	55[b]	172[b]	195[c]
Elongation at max stress, %	5[b]	22[b]	80[c]

[a]Column headings indicate propellant type and batch number.
[b]These properties were reported to improve greatly with longer cure time at 160°F.
[c]Cure time and mechanical properties near optimum.
[d]*CBS 24, 40, 45, 46, 47,* and *57.*

Table 2. Composition and initial properties of polyurethane propellants[a]

Composition, wt %	X-500-1 S-102	X-532 S-100	X-535 S-101	X-600 PD-79
Ammonium perchlorate, ground	56.00	56.00	56.00	55.87
Ammonium perchlorate, unground	24.00	24.00	24.00	23.94
Lithium perchlorate	—	—	—	0.19
Polypropylene glycol 2025	17.74	16.82	17.20	13.31
P-II polymer[b]	—	—	—	5.03
1,2,3-Trimethylol propane	0.12	0.26	0.09	0.09
Alrosperse 11p[c]	—	0.50	0.50	—
Phenyl-β-naphthylamine	0.25	0.25	0.25	0.25
Ferric acetylacetonate	0.05	0.04	0.04	0.01
2,4-Toluene diamine	1.84	2.11	1.92	1.31
Cure conditions				
Cure temperature, °F	140	140	140	180[d]
Cure time, hours	72	72	72	88[d]
Measured initial mechanical properties at 77°F				
Tensile strength, psi	117.3	118.8	112.3	152.2[d]
Elongation at max load, %	24.2	44.8	91.8	40.6[d]

[a]Column headings indicate propellant type and batch number.
[b]Polymer prepared from 2 moles of polypropylene glycol, 4 moles of 2,4-toluene diisocyanate, and 1 mole of 2,4-toluene diamine.
[c]Wetting agent by Geigy Industrial Chemicals.
[d]Undercured under these conditions; completion of cure by holding at 120°F for 2 weeks gives a tensile strength of 180 to 200 psi and an elongation at maximum load of about 35%.

charges were cooled, cut, and milled into standard dumbbell specimens (Ref 5), and initial tensile properties were measured the same day. The remaining specimens were suspended in tightly-sealed 2-gallon metal paint cans, each containing about one liter of an appropriate conditioning solution to give the desired humidity. A separate can was used for each propellant to prevent the diffusion of gaseous products from one propellant type into another. This effect was only noticeable with the polysulfides, where the cover and walls of the can became coated with a deposit of phenylene diamine, which is a product of the curing reaction discussed later. The moisture content of the cans was checked at frequent intervals with an Alnor dew point tester.

The conditioning solutions are listed in Table 3. Average measured humidities agreed reasonably well with nominal values listed in handbooks, except for the unsaturated $CaCl_2$ solutions and for all systems with a nominal relative humidity of 80%. The reason for the latter discrepancy lies in the measurement, since the Alnor instrument is not well suited to determine dew points which are close to ambient temperatures. The $CaCl_2$ solutions presumably failed to give the desired relative humidity because the water content analysis of the hydrated salt was in error. The values in the last column of Table 3 are used to identify the humidity conditions during storage. Since relative humidities vary greatly with dry bulb temperature, it is estimated that these values may be in error by about ±15% of the listed figure. The unsaturated solutions of glycerol and $CaCl_2$ were used only with the X-532 propellant; the saturated salt solutions were employed as the humidity conditioning agents with all other propellants.

Table 3. Moisture content of surrounding atmosphere during propellant storage

Nominal relative humidity at 77°F, %	Conditioning agent	Concentrations of solutions, wt %	Average measured dew point, °F	Average measured humidity, %	
				At 77°F	At 79°F
0	$CaSO_4$	Anhydrous	−18	2	2
Ambient	—	—	28	17	15
20	Glycerol	90.4	35	22	20
31	$CaCl_2 \cdot 6H_2O$	Sat	43	29	28
40	$CaCl_2$	39.6	42	28	27
40	Glycerol	78.4	54	44	42
47	$LiNO_3 \cdot 3H_2O$	Sat	55	46	43
57	$NaBr \cdot 2H_2O$	Sat	60	56	52
60	$CaCl_2$	31.7	57	49	46
60	Glycerol	61.9	62	59	55
79	NH_4Cl	Sat	66	69	65
80	$CaCl_2$	22.3	65	66	62
80	Glycerol	42.1	67	71	66
100	Dist water	100	—	—	—

The containers and one additional set of dumbbell specimens were stored in a controlled-atmosphere chamber at an average temperature of 79 ±4°F and relative humidity of 15 ± 5%. Duplicate specimens were withdrawn after 1, 4, 7, 14, 28, and 50 days of storage and tested immediately on an Instron tester under ambient conditions of temperature (77 ±4°F) and humidity. The jaw separation rate was 2 in./min (strain rate 0.74 min^{-1}). Only the tensile strength S_m and elongation at maximum load e_m have been calculated.

2. Results

Figure 3 shows the tensile strength and elongation of JPL 138 polysulfide propellant vs storage time at 79°F and various humidities. The results for JPL 128 and 136 are similar in character. Each point represents an average of at least two tensile tests, and all experimental points are shown. The mechanical properties of all three propellants improved greatly during ambient storage at low and intermediate humidities. This suggests the possibility that the propellants were not fully cured during the oven cycle given in Table 1. The normal cure of liquid polysulfide polymers by *p*-quinone dioxime is effected by oxidation of thiol linkages to disulfides:

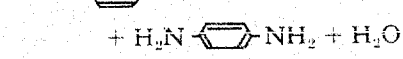

$$\text{HON}\!=\!\bigcirc\!=\!\text{NOH} + \text{HSRSH} \rightarrow \text{H(SRS)}_x\text{H} + \text{H}_2\text{N}\!-\!\bigcirc\!-\!\text{NH}_2 + \text{H}_2\text{O}$$

Sulfur, when included in the formulation, produces additional cure through a similar reaction with the evolution of hydrogen sulfide:

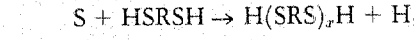

$$\text{S} + \text{HSRSH} \rightarrow \text{H(SRS)}_x\text{H} + \text{H}_2\text{S}$$

Since the initial polymer is branched, crosslinking occurs by the same mechanism. Not all of the thiol end groups are consumed in this process, and it has been postulated (Ref 7) that oxygen diffuses into the propellant and oxidizes more of the thiol to disulfide, causing additional chain extension and crosslinking and resulting in improved mechanical properties. Since water is liberated in the reaction, it could be expected that such a secondary cure would be accelerated in a dry atmosphere and inhibited by moisture due to a mass action effect. However, earlier work at this Laboratory (Ref 17) showed that JPL 128 propellant cures at nearly equal rates in dry nitrogen or in dry air and that the effect of atmospheric oxygen on the rate and extent of the curing reaction is probably negligible. At the same time it was shown that optimum physical properties are achieved only when the water

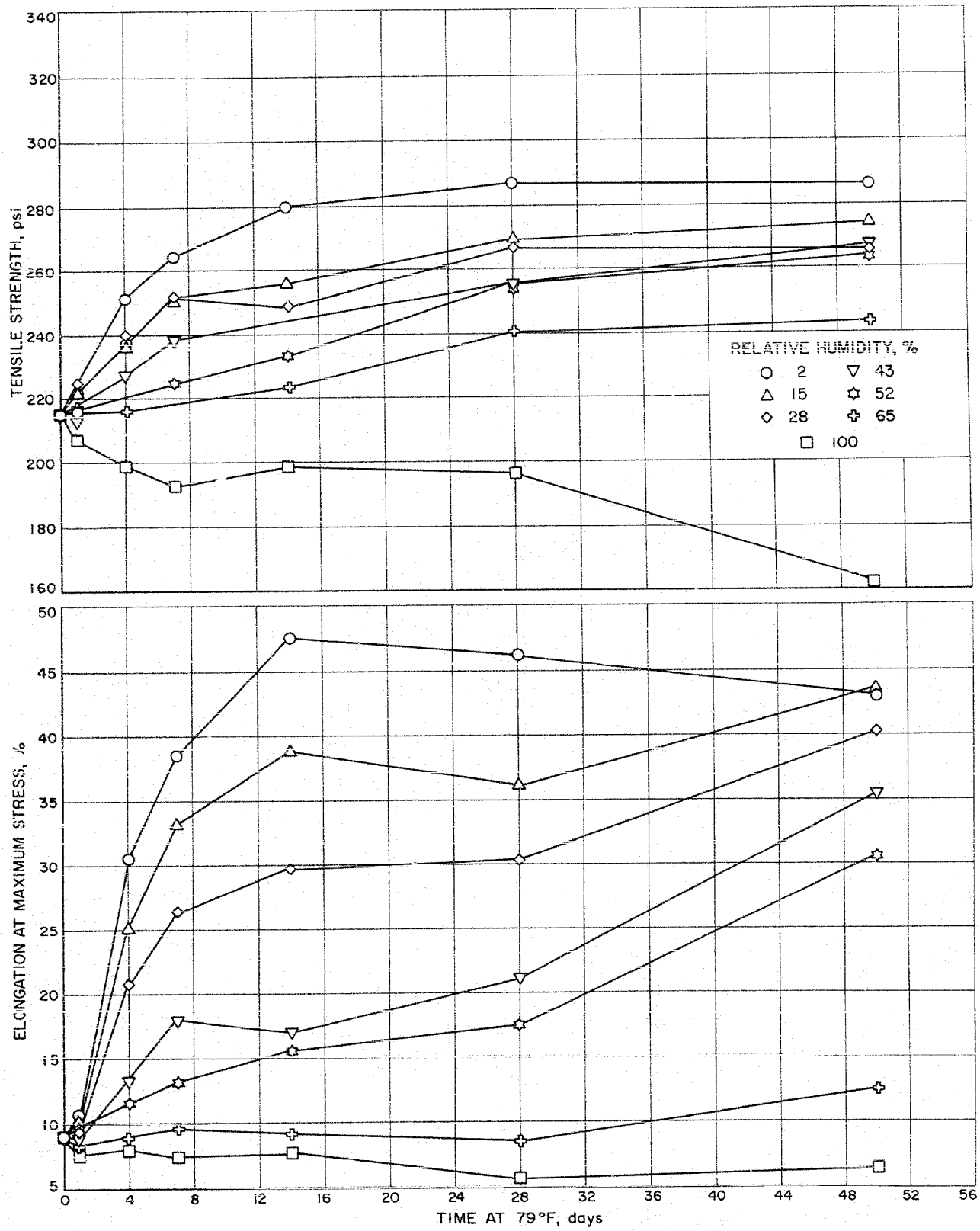

Figure 3. Tensile strength and elongation at maximum stress of JPL 138 propellant during ambient aging at various humidities

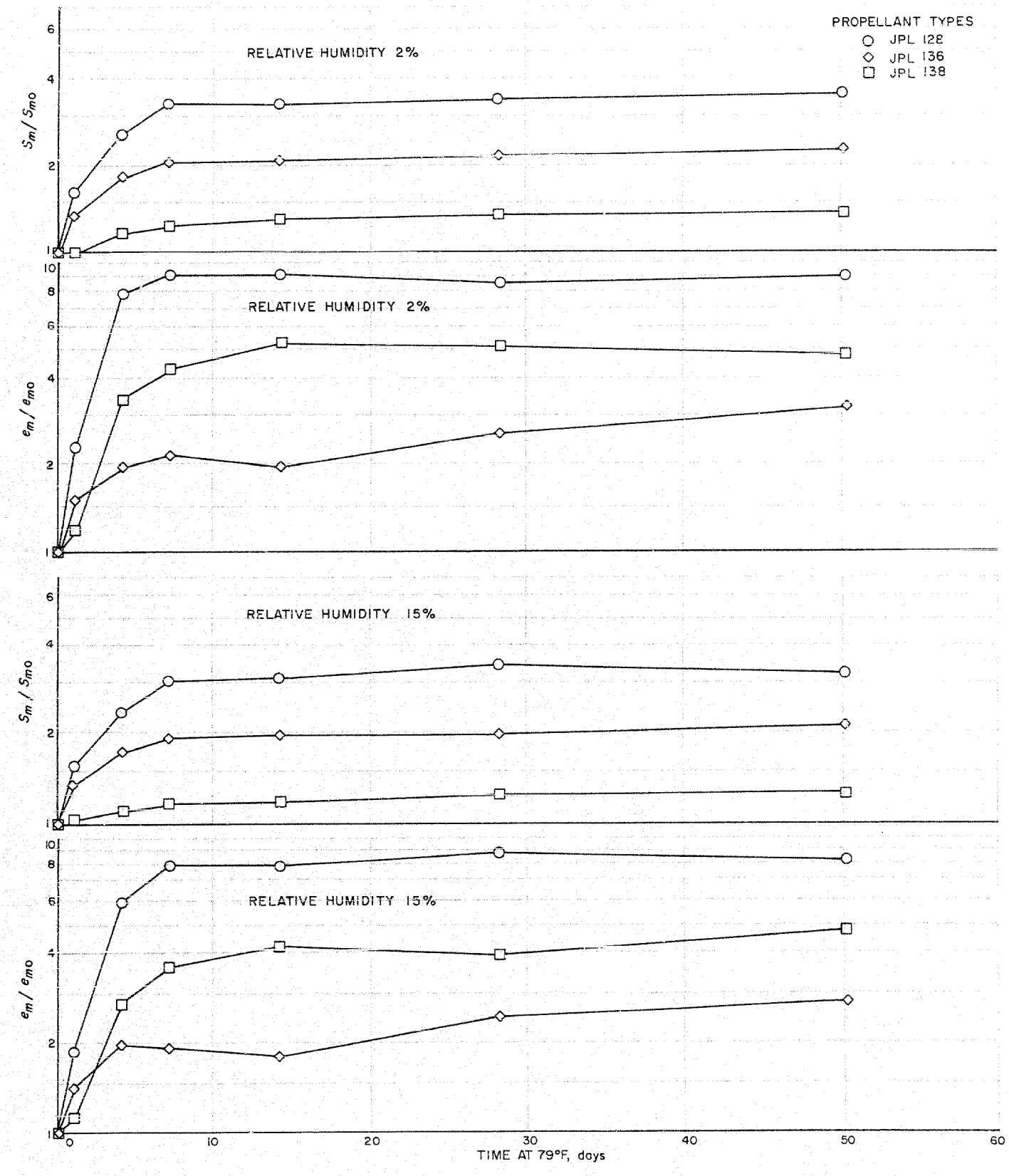
PROPELLANT TYPES
JPL 128
JPL 136
JPL 138
RELATIVE HUMIDITY 2%
S_m / S_{mo}
RELATIVE HUMIDITY 2%
e_m / e_{mo}
RELATIVE HUMIDITY 15%
S_m / S_{mo}
RELATIVE HUMIDITY 15%
e_m / e_{mo}
TIME AT 79°F, days

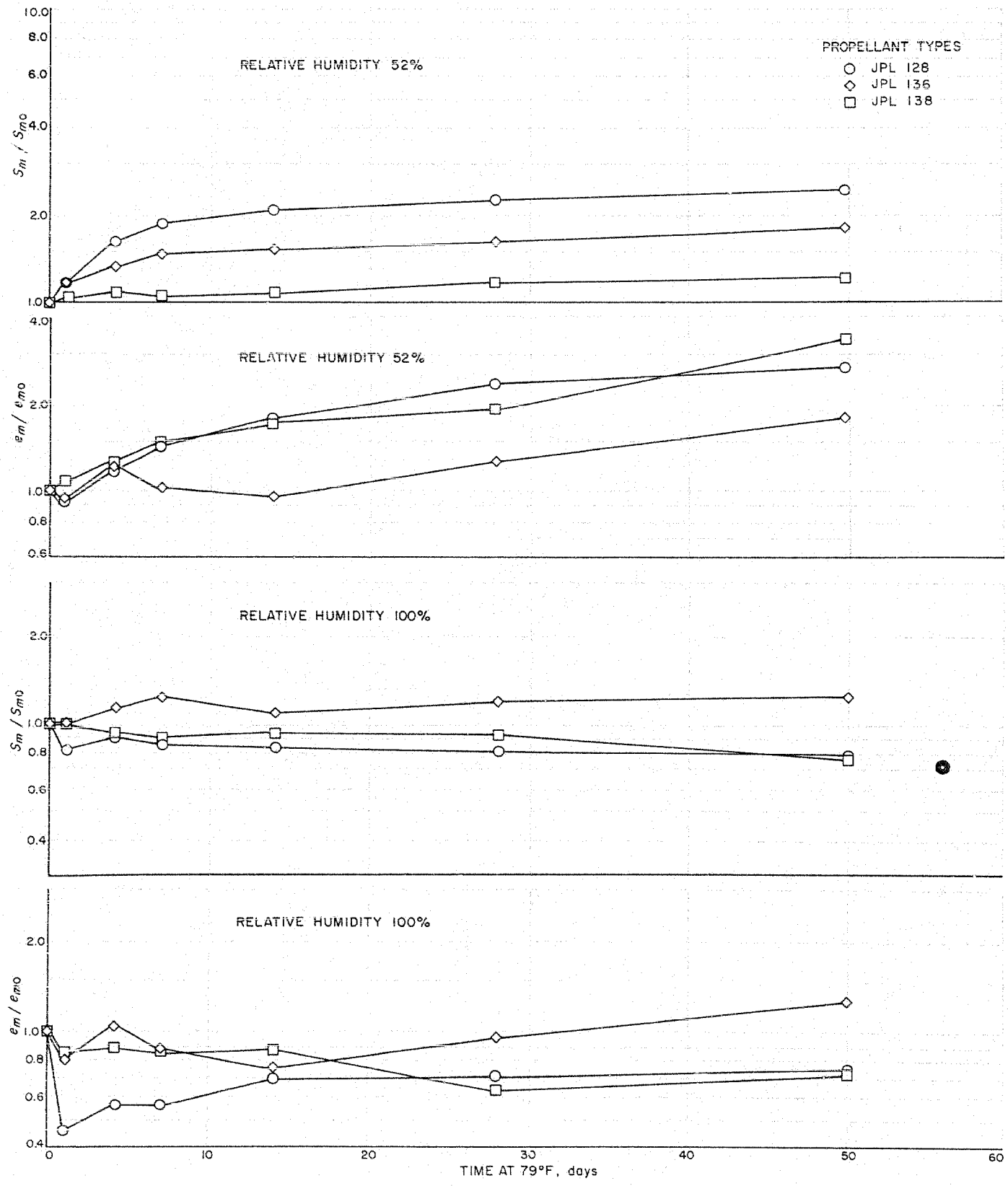

Figure 4. Properties of polysulfide propellants during ambient aging at various relative humidities

formed in the polymerization of polysulfide fuels is allowed to diffuse out through the propellant surface. This process is again a function of the moisture content of the surrounding atmosphere, but does not require the presence of oxygen.

Results of the present study could be explained by either of these mechanisms, since no effort was made to exclude oxygen. The rate at which the mechanical properties improve with time, as well as the maximum values of tensile strength and elongation reached, are seen to be greatly dependent on the moisture content of the surrounding atmosphere. In a saturated atmosphere, no water diffusion from the propellant is possible and actually some decrease in mechanical properties is observed.

The characteristics of the tensile curves change markedly during storage at low humidities. Before aging, the nominal stress increases with strain to a maximum value at the yield point, and further elongation takes place under decreasing stress. As aging at low humidities progresses, the values of stress and strain at yield point increase gradually, until no yield point is observed and the strain at maximum load becomes nearly identical with the strain at break. The Shore hardness also increases during aging, though not to such a great extent as the tensile properties. Further conclusions may become apparent when the stress and strain at break, as well as the hardness values, are systematically tabulated.

The mechanical properties of the three polysulfide propellants vary at different rates during storage, as is seen when the data are replotted as the ratio of aged to initial properties. Figure 4 shows the results at four selected humidity levels. The following general observations can be made: (1) The JPL 128 propellant shows the greatest and most rapid relative improvement in both tensile strength and elongation during storage, with optimum values being obtained in about 7 days in a dry atmosphere. This propellant also has the largest loss in properties at 100% humidity. This is not surprising, since the propellant contains no sulfur and the entire cure is accompanied by the evolution of water. Thus JPL 128 would be expected to contain more water after cure and to be more dependent on its removal for the development of optimum properties. (2) The JPL 136 propellant exhibits an intermediate increase in tensile strength, which requires about 2 weeks at low humidity to reach a maximum value. Its elongation, however, increases at the slowest rate during the entire 50-day storage period. (3) The JPL 138 propellant reaches maximum elongation in 2 weeks of ambient storage at low humidity. Its tensile strength, which was the highest of the three polysulfide propellants after oven cure, shows the least amount of increase. Both JPL 136 and JPL 138 are presumed to be partially cured by *p*-quinone dioxime and partially by sulfur. The latter reaction does not generate water, and consequently the extent of reaction is independent of moisture in the surrounding atmosphere.

Approximate values for mechanical properties after the initial oven cure and after aging at ambient temperature in a dry atmosphere for the three polysulfide propellants are shown in Table 4.

Data for the polyurethane propellants, illustrated with data for X–535 and X–600 as shown in Figures 5 and 6, indicate an entirely different effect of various humidity environments. Propellants stored in a dry atmosphere show little or no change in mechanical properties within experimental error. At higher humidities, *both* the tensile strength and the strain at maximum stress decrease markedly, the extent of the change being roughly proportional to the moisture content of the surrounding atmosphere. This is in contrast to the effects of aging at high temperatures or of formulation changes, which tend to give a decrease in tensile strength but an increase in elongation (Ref 5, Ref 15, and references in the latter). It is particularly important to note how rapidly the deterioration of mechanical properties takes place. The maximum decrease occurs during the first 24 hours of storage, after which the values drop off at a decreasing rate. At relative humidities up to about 60%, the mechanical properties of all four polyurethane propellants appear to reach an equilibrium value within 2 weeks. This suggests that the effect is due to physical absorption of water into the propellant rather than to chemical degradation of the binder. In a saturated atmosphere, however, the tensile strength continues to decrease, while the elongation at maximum stress goes through a minimum and then increases. It was also observed qualitatively that the ultimate strain of propellants stored at 100% humidity increases with time, in agreement with previously reported results (Refs 7 and 13). The tensile curves frequently show a second maximum after the initial yield point. The specimens appear to be saturated with water, and some extraction of the oxidizer takes place. Since the deliquescence point of ammonium perchlorate occurs at about 95% relative

Table 4. Mechanical properties of polysulfide propellants before and after ambient storage in a dry atmosphere

Propellant	Tensile strength, psi		Elongation at max stress, %	
	Initial	Final	Initial	Final
JPL 128	60	195	7	60
JPL 136	85	185	10	33
JPL 138	215	285	9	45

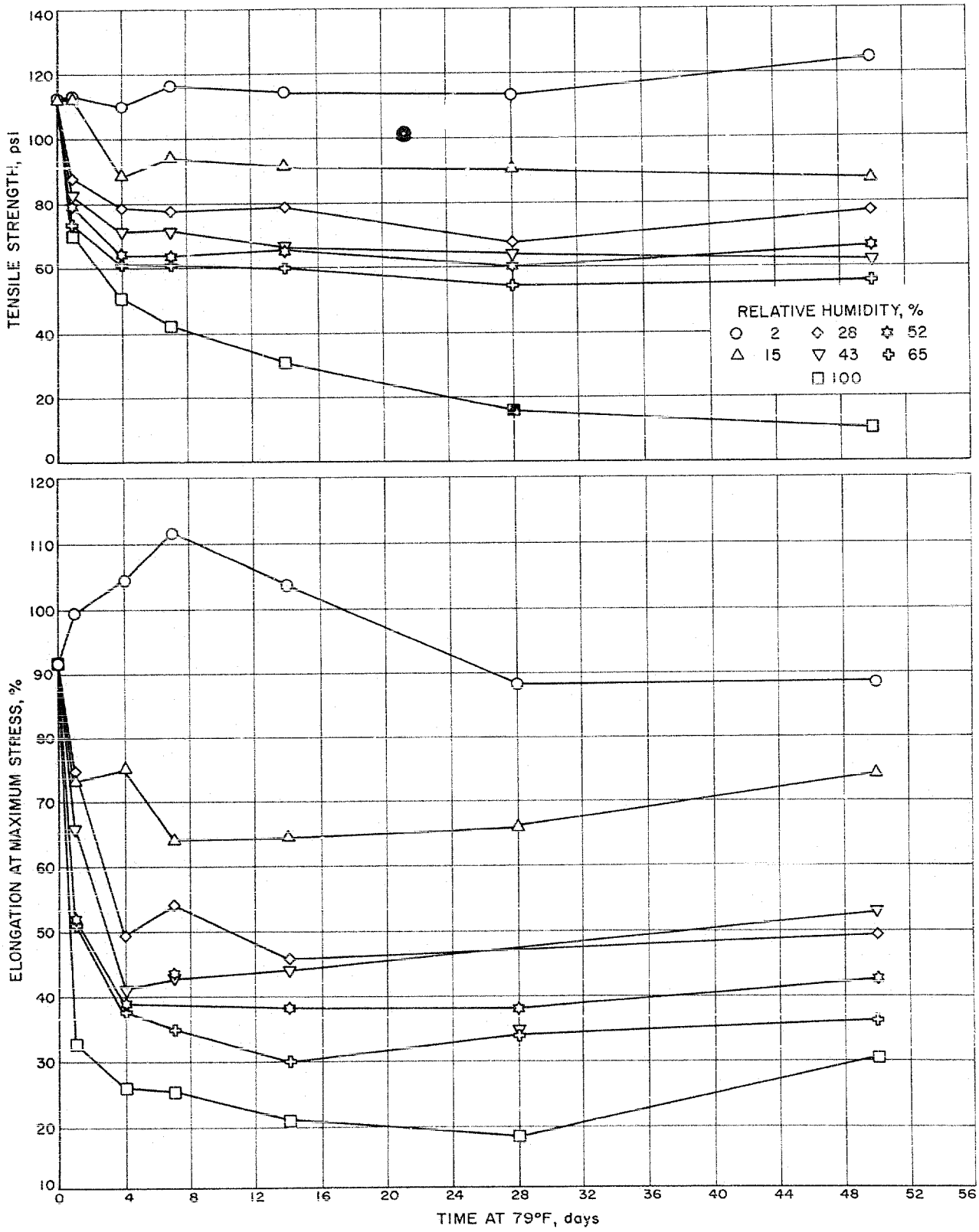

Figure 5. Tensile strength and elongation at maximum stress of JPL X-535 propellant during ambient aging at various humidities

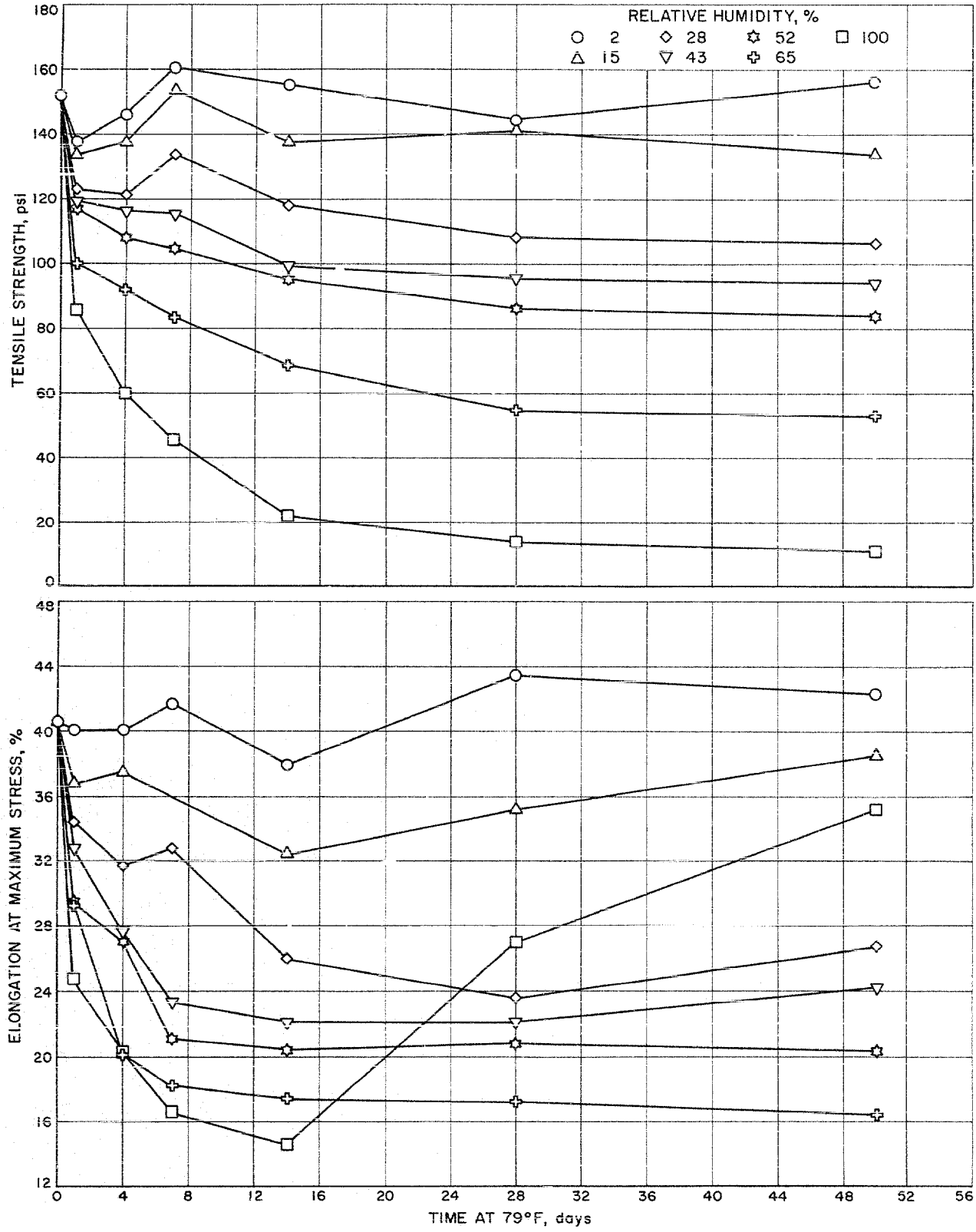

Figure 6. Tensile strength and elongation at maximum stress of JPL X-600 propellant during ambient aging at various humidities

humidity at 79°F (Ref 8), an entirely different mechanism of water absorption in saturated air could be anticipated.

Examination of the same data, replotted in Figure 7 on a relative basis but showing only 4 humidities, leads to the following conclusions: (1) The X-500-1 propellant is least affected by atmospheric moisture under most environmental conditions, and the X-600 propellant is second best. It is notable that these propellants do not contain a wetting agent. (2) The propellants prepared with Alrosperse 11p show the greatest decrease in mechanical properties during storage in moist atmospheres. The X-535 propellant, which had best mechanical properties initially, is most severely affected.

B. Volume Changes Under Tensile Deformations

In tensile testing of composite propellants, the quantity S_m is the maximum value of stress (usually called the tensile strength) and the quantity e_m is the strain at maximum stress. With most propellants, further elongation past this yield point takes place under decreasing stress, because the oxidizer has separated from the binder with the formation of vacuoles and thus has no further reinforcing effect. Previous work at this Laboratory has shown that some separation of oxidizer and resin occurs before e_m is reached, and it was believed that it begins rather abruptly at some critical value of strain e_c which is roughly equal to $\frac{2}{3}\ e_m$ (Ref 18). Thus e_c rather than e_m may be a more realistic failure criterion to be used in the design of case-bonded solid rocket motors.

The formation of vacuoles between oxidizer and binder necessarily results in a volume increase of the propellant specimen, which can be measured in a dilatometer. Such a study was carried out with glass bead–polyvinylchloride composites (Ref 19), but the work was not extended to actual propellant formulations. The dilatometer used in the previous study is not suitable for use with propellants for the following reasons:

(1) Propellants cannot be prepared in the required form of elongated-ring specimens.
(2) Precision of the apparatus at small volume changes is unsatisfactory, due to leakage or flexibility of the O-ring seal.
(3) The dilatometer cannot be used to study volume changes as a function of time.

A new apparatus was devised for the measurement of volume changes of composite propellants during extension.

1. Test Apparatus and Operations

The new device, shown in Figure 8, determines the volume of propellant specimens gravimetrically by measuring their weight when immersed in an inert liquid of known density. The weighing unit is a simple Jolly balance with a calibrated fine spiral steel spring, which has a sensitivity of about ±2 mg. The liquid is a Dow-Corning DC-200 silicone oil with a viscosity of about two centistokes at room temperature. This fluid does not swell the polyurethane resin-binder or dissolve the ammonium perchlorate oxidizer, yet it is of sufficiently low viscosity to wet the specimens readily and completely. No appreciable penetration of the silicone fluid into propellants was observed during long periods of immersion; in a few isolated instances, however, some extraction of excess catalyst or the antioxidant took place as evidenced by discoloration of the oil and by a slight weight loss of the propellant samples. The container of silicone fluid is surrounded by a constant-temperature bath controlled thermostatically within ±0.2°C.

The propellant specimens are rings 0.25 inch wide with an inside diameter of 2.25 inches and an outside diameter of 2.5 inches, as shown in Figure 9. The rings are cut on a lathe from a propellant tube, which is prepared by casting and curing in a specially-constructed tubular mold. The casting of propellant tubes is somewhat painstaking and difficult, but can be accomplished successfully with most conventional polysulfide and polyurethane propellants. The dimensions of the specimens are determined accurately with a conical plug gage and a standard thickness gage (Fig 9).

The figure also shows the mandrels used to extend the propellant rings to strains ranging from 0.05 to 0.35, based on the inside diameter of the ring. It is true that the inside and outside of a ring are not stretched equally by this method, but the error is minimized by making the ratio of outside to inside diameter small (1.11). The upper section of each mandrel is conical to permit smooth and rapid extension of the propellant rings, and the lower cylindrical section has a diameter calculated to give the desired strain. The aluminum mandrels are hollow, and their bulk density is adjusted to exceed slightly the density of the silicone oil at the test temperature. The weight and volume of each mandrel are accurately known. Each immersed mandrel puts only a slight load on the Jolly balance spring and permits high precision in determining the volume of the stretched propellant.

To make a measurement, a propellant ring of known dimensions, weight, and volume is extended rapidly by

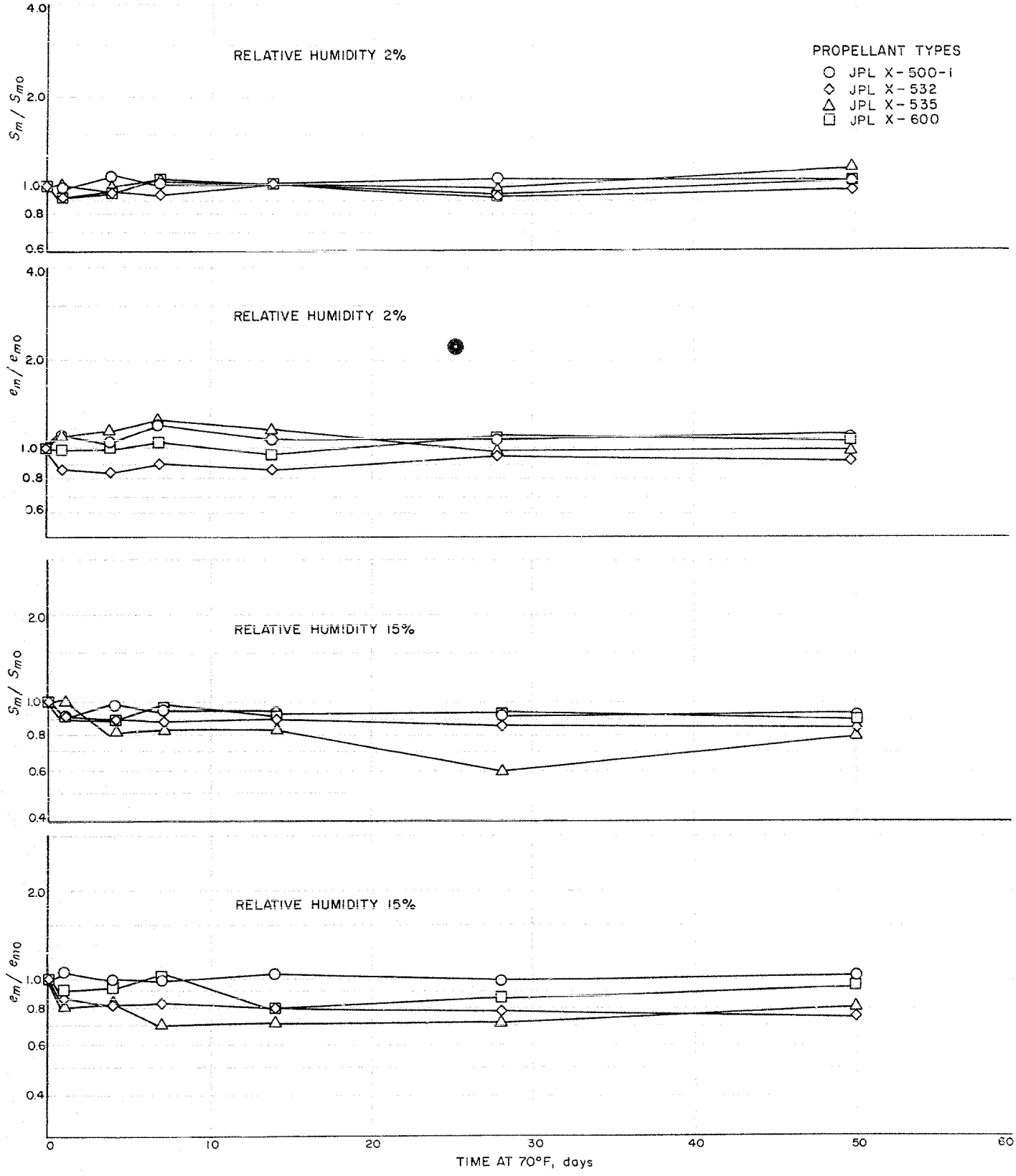
RELATIVE HUMIDITY 2%
PROPELLANT TYPES
JPL X-500-i
JPL X-532
JPL X-535
JPL X-600
S_m / S_{mo}
RELATIVE HUMIDITY 2%
e_m / e_{mo}
RELATIVE HUMIDITY 15%
S_m / S_{mo}
RELATIVE HUMIDITY 15%
e_m / e_{mo}
TIME AT 70°F, days

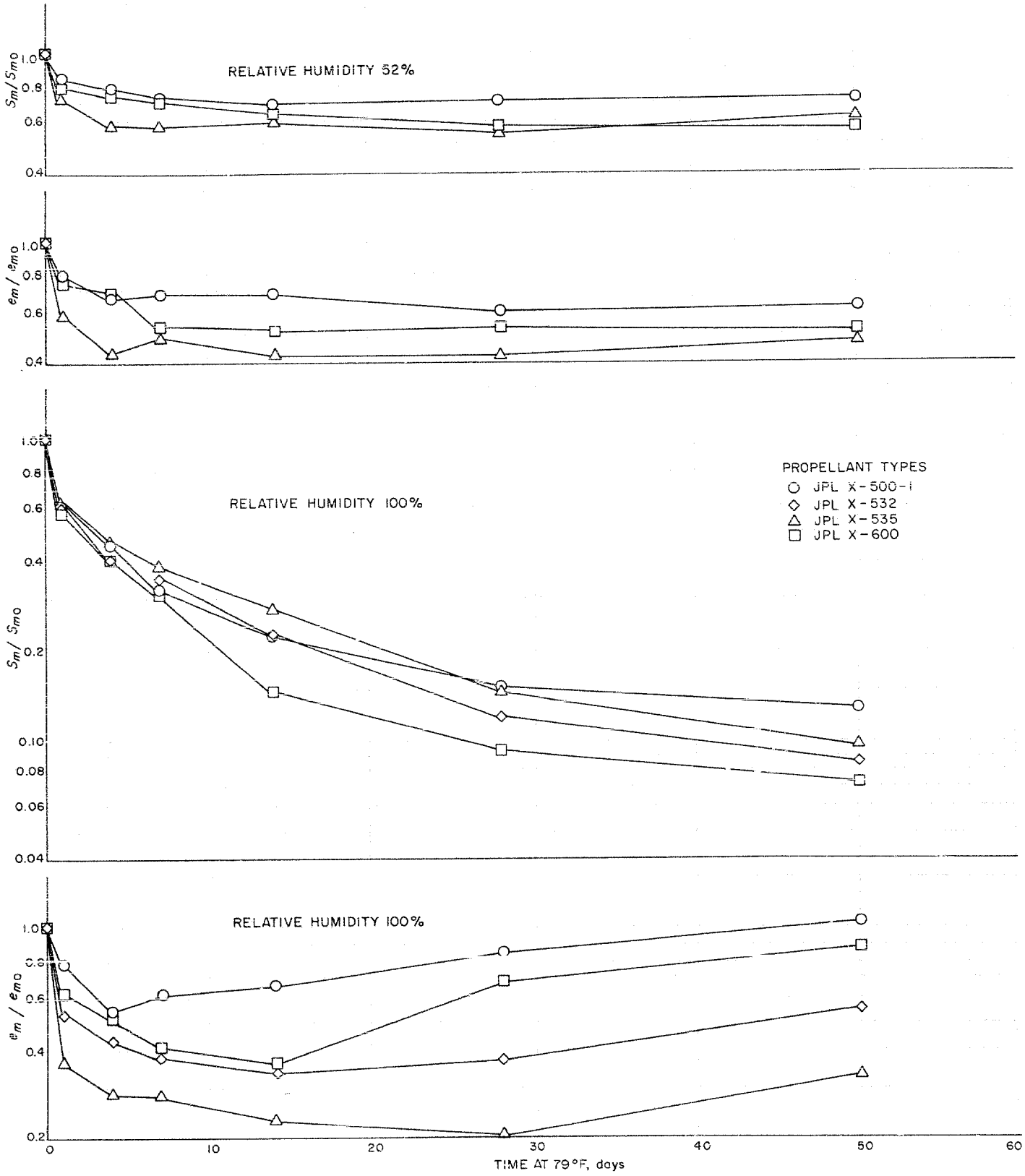

Figure 7. Properties of polyurethane propellants during ambient aging at various relative humidities

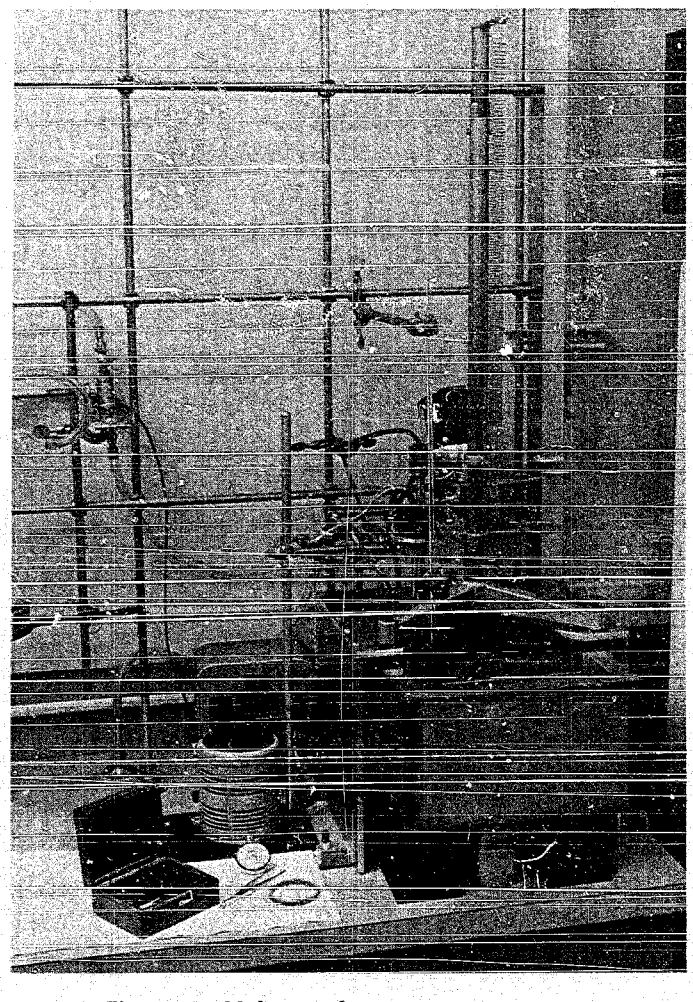

Figure 8. Volume-change test apparatus

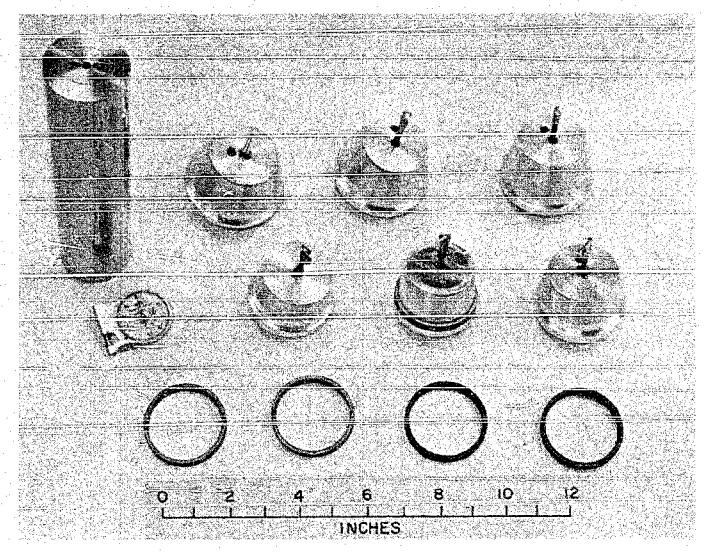

Figure 9. Volume-change test specimens and strain mandrels

sliding over the appropriate mandrel, as shown in one example in Figure 9. The assembly is suspended from the Jolly balance spring in the silicone oil, and readings of apparent weight are taken as a function of time. From these data, changes in volume (if any) with time can be calculated for any one value of strain. After an equilibrium volume is reached, the ring is removed from the mandrel and the extent of volume recovery is measured.

2. *Test Results*

After numerous experimental difficulties, the apparatus now appears to be working satisfactorily and to give reproducible and meaningful results. Recent data obtained with two polyurethane propellants have not yet been reduced. However, it can be said that the existence of the critical strain e_c has not been confirmed with these propellants. The samples were found to increase in volume at all strains from 5 to 35%. Preliminary log-log plots of the volume ratio V/V_0 versus the extension ratio $\alpha = L/L_0$ are decidedly non-linear, indicating that the Poisson's ratio defined in terms of the logarithmic strain decreases continuously with strain. This finding differs from conclusions reported previously as a result of work with glass bead composites (Ref 19).

C. Motor Strain Testing

A great deal of effort has been expended studying the physical properties of solid propellants under uniaxial loading. At the same time attempts have been made to extend the results of these one-dimensional tests to predict the behavior of the grain in a multi-axial stress state such as occurs in an operational environment. Unfortunately, the applicability of this correlation has never been successfully demonstrated.

Attention should be directed to an evaluation of the response of the grain to the imposition of multi-axial stresses with particular emphasis on those design criteria which would contribute to crack inception upon thermal cycling or rapid pressurization due to ignition.

One model under investigation as a device to study the mechanical behavior of composite solid propellants in other than the usual one-dimensional uniaxial tension tests is the hollow cylindrical section of propellant, case-bonded in a thin-walled chamber. Motors with various

web thicknesses will be pressurized internally and these motors will also be thermally cycled in a subsequent series of tests to investigate thermal loading effects.

1. Theoretical Discussion

This section presents the theoretical elastic stresses and strains which are expected from internal pressurization for the various parameters involved. The parameters of interest are: the modulus and Poisson's ratio of the propellant, the geometrical configuration of the grain, and the case properties. The treatment is based on small-deformation elastic theory, and it is felt that localized maximum strains of the order of 20 to 40% will give fairly reasonable engineering trends. This is particularly true of the above model in which high straining is quite localized in the inner radius region.

Two different derivations of the elastic equations are given. The first, referred to as the three-dimensional model, includes the axial elongation effect due to internal pressure acting on the ends. The propellant was assumed to be cast completely up to the ends and bonded there transmitting pressures to the end plates. The end plates, in turn, pull axially on the case which is countering this tendency through radial expansion from internal pressure. In the actual tests, the propellant will not be bonded to the ends and will experience axial compression at the ends. However, the motor is sufficiently long so as to minimize this end effect within the mid-section, experiencing loads close to those given by the end-bonded model.

The second derivation, referred to as plane strain, assumes the axial strain is zero. Results from the above three-dimensional analysis validate this assumption. The consequent hoop stresses and strains are very close to those from the three-dimensional model, being off by only a few percent in the incompressible region.

A convenient parameter $\mathcal{E}_c$, relating case modulus to propellant modulus is introduced.

$$\mathcal{E}_c = \frac{(b/a)^2}{(b/a)^2 - 1} \cdot \frac{2\,b\,E_c}{b\,E} = \frac{6.03 \times 10^5}{E} \cdot \frac{(b/a)^2}{(b/a)^2 - 1} \qquad (1)$$

where a is the inside radius, b the outside radius, E is Young's modulus, and h is the case thickness.

a. Elastic model. Elastic small-deformation theory is used to predict the stresses and strains which might be experienced in a cylindrical propellant grain bonded to an elastic case under internal pressure. The approach used is to specify stresses which match boundary conditions, then determine strains and displacements requiring that at the bonded surfaces the stresses and displacements match between the propellant and case. It is emphasized that the results are reasonably accurate only for small strains and begin to deteriorate with large strains.

The choice of a simple model to facilitate the analysis, yet retain certain features of interest, led to the following:

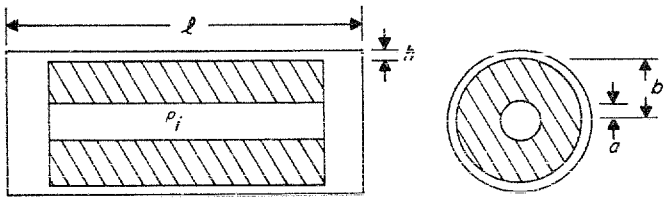

The propellant is bonded to the outer case and to the ends. The case is considered thin ($h << b$), while the ends are rigid and exert an axial tension on the case due to internal pressure acting on the grain. However, the cylindrical case is free to expand radially, and equally up to the ends.

Under internal pressure the outer case shell and propellant being bonded move together and experience a pressure $p_o\,(\sigma_r|_{r=b} = -p_o)$. In a similar manner the ends experience a pressure $p'\,(\sigma_z = -p')$. Since the analysis is valid only for small strains, it does have practical value in application to higher modulus, lower elongation propellants.

b. Derivation of equations. The boundary conditions on stresses and displacements are radial stress on inside periphery of grain

$$\sigma_r|_{r=a} = -p_i$$

radial stress with no pressure on outside

$$\sigma_r|_{r=b+h} = 0$$

radial displacements of propellant and case equal at bond

$$u|_{r=b} = u_c|_{r=b}$$

axial displacements of propellant and case equal at bond

$$w|_{z=0,\,l} = w_c|_{z=0,\,l} \qquad (2)$$

Stresses in a hollow propellant tube due to radial pressures p_i on inside and p_o on outside along with axial pressure p' are radial stress

$$\sigma_r = \frac{A}{r^2} + 2C$$

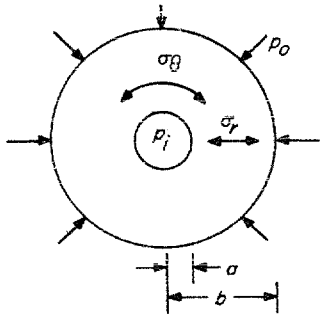

hoop stress

$$\sigma_\theta = \frac{-A}{r^2} + 2C$$

axial stress

$$\sigma_z = -p' \qquad (3)$$

where

$$A = \frac{a^2 b^2 (p_o - p_i)}{b^2 - a^2}$$

$$2C = \frac{p_i a^2 - p_o b^2}{b^2 - a^2} \tag{4}$$

Stresses are positive when in tension, negative in compression.

The strains in the propellant are determined from the stresses by

$$\varepsilon_r = \frac{1}{E}[\sigma_r - \nu(\sigma_\theta + \sigma_z)] \tag{5}$$

and similar formulas for ε_θ and ε_z by commuting stresses. Explicitly, the strains are

$$\varepsilon_{\binom{r}{\theta}} = \frac{1}{E}\left[\pm\frac{(1+\nu)A}{r^2} + (1-\nu)2C + \nu p'\right]$$

$$\varepsilon_z = -\frac{1}{E}[p' + 4\nu C] \tag{6}$$

where the upper sign choice is for ε_r and lower for ε_θ.

The displacements of the propellant are given by

$$u = \int \varepsilon_r\, dr = r\varepsilon_\theta = \frac{1}{E}\left[-\frac{(1+\nu)A}{r} + (1-\nu)2Cr + \nu p' r\right]$$

$$w = \int \varepsilon_z\, dz = -\frac{1}{E}[p' + 4\nu C]\, z \tag{7}$$

assuming the temperature uniform throughout.

Proceeding on to the case, the stresses for a thin wall are

$$\sigma_{\binom{r}{\theta}} = B\left(1 \mp \frac{b^2}{r^2}\right) \quad B = \frac{b p_o}{2b}$$

$$\sigma_z = p'' = \frac{(b^2 - a^2)p' + a^2 p_i}{2bb} \tag{8}$$

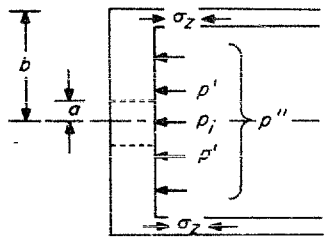

where the total pressure on the end is transmitted into tension of the outer shell. This ignores localized bending in the neighborhood of the junction; however, it does include the flexibility of radial expansion as is somewhat the situation in both the head and nozzle ends.

The strains in the case are

$$\varepsilon_{\binom{r}{\theta}} = \frac{1}{E_c}\left[\mp\frac{(1+\nu_c)Bb^2}{r^2} + (1-\nu_c)B - \nu_c p''\right]$$

$$\varepsilon_z = \frac{1}{E_c}[p'' - 2\nu_c B] \tag{9}$$

The displacements of the case are

$$u_c = \frac{1}{E_c}\left[\frac{(1+\nu_c)Bb^2}{r} + (1-\nu_c)Br - \nu_c p'' r\right]$$

$$w_c = \frac{1}{E_c}[p'' - 2\nu_c B]\, z \tag{10}$$

Upon equating $u = u_c$ at $r = b$ and $w = w_c$, expressions for p_o and p' as functions of internal pressure p_i are obtained.

$$\left.\begin{aligned} p_o &= \frac{\{2(1-\nu^2)\mathcal{E}_c^2 + [2 - \nu + \nu_c(1-2\nu)]\mathcal{E}_c\}\, p_i}{(1+\nu)\left\{(1-2\nu)\frac{b^2}{a^2} + 1\right\}\mathcal{E}_c^2 + \left\{[3 - \nu(1+4\nu_c)]\frac{b^2}{a^2} + (1+\nu)\right\}\mathcal{E}_c + 2(1-\nu_c^2)\frac{b^2}{a^2}} \\ p' &= \frac{\left[2\nu\left\{(1+\nu)\left(\frac{b^2}{a^2} - 1\right)\right\}\mathcal{E}_c^2 + \left\{\left[-(1+3\nu) + 2\nu_c(2+\nu)\right]\frac{b^2}{a^2} - (1+\nu)\right\}\mathcal{E}_c - 2(1-\nu_c^2)\frac{b^2}{a^2}\right] p_i}{\left[\frac{b^2}{a^2} - 1\right]\left[(1+\nu)\left\{(1-2\nu)\frac{b^2}{a^2} + 1\right\}\mathcal{E}_c^2 + \left\{[3 - \nu(1+4\nu_c)]\frac{b^2}{a^2} + (1+\nu)\right\}\mathcal{E}_c + 2(1-\nu_c^2)\frac{b^2}{a^2}\right]} \end{aligned}\right\} \tag{11}$$

Other stresses and strains are obtained by substituting the previous expressions into the earlier equations. The case-modulus parameter is

$$\mathcal{E}_c = \frac{2\dot{b}bE_c}{(b^2 - a^2)E} = \frac{2(b/a)^2}{(b/a)^2 - 1} \cdot \frac{\dot{b}}{b} \cdot \frac{E_c}{E} \tag{12}$$

The stress on inner radius of the propellant due to internal pressure is

c. Plane strain. The axial strain is quite small under internal pressurization. Therefore, a good approximation results from assuming no axial straining, a condition, referred to as plane strain. This analysis will yield the quantities p_o, $\sigma_\theta|_{r=a}$, $\varepsilon_\theta|_{r=a}$, and $\varepsilon_\theta|_{r=b}$, which are almost identical with those from the three-dimensional model, but, of course, will not give p' or ε_z.

$$\sigma_\theta|_{r=a} = \frac{1}{(b/a)^2 - 1}\left[\frac{\begin{array}{c}(1+\nu)\{(1-2\nu)(b/a)^4 - 2(1-\nu)(b/a)^2 + 1\}\mathcal{E}_c^2 \\ +\{[3-\nu(1+4\nu_c)](b/a)^4 + 2(\nu-\nu_c)(b/a)^2 + (1+\nu)\}\mathcal{E}_c + 2(1-\nu_c^2)(1+(b/a)^2)(b/a)^2\end{array}}{(1+\nu)[(1-2\nu)(b/a)^2+1]\mathcal{E}_c^2 + \{[3-\nu(1+4\nu_c)](b/a)^2 + (1+\nu)\}\mathcal{E}_c + 2(1-\nu_c^2)(b/a)^2}\right] p_i \tag{13}$$

The strain and displacement on inner radius are

$$\left.\begin{matrix}\varepsilon_\theta|_{r=a} \\ \dfrac{v}{\dot{a}}\Big|_{r=a}\end{matrix}\right\} = \frac{1}{E[(b/a)^2-1]}\left[\frac{\begin{array}{c}(1+\nu)^2(1-2\nu)[(b/a)^2-1]^2\mathcal{E}_c^2 + (1+\nu)\{[3-\nu(1+4\nu_c)](b/a)^4 \\ -[\nu+2\nu_c(1-3\nu)](b/a)^2 + (1-2\nu)\}\mathcal{E}_c + 2(1-\nu_c^2)[(1+\nu)(b/a)^2 + (1-2\nu)](b/a)^2\end{array}}{(1+\nu)[(1-2\nu)(b/a)^2+1]\mathcal{E}_c^2 + \{[3-\nu(1+4\nu_c)](b/a)^2 + (1+\nu)\}\mathcal{E}_c + 2(1-\nu_c^2)(b/a)^2}\right] p_i \tag{14}$$

The strain and displacement on outer radius are

$$\left.\begin{matrix}\varepsilon_\theta|_{r=b} \\ \dfrac{v}{\dot{b}}\Big|_{r=b}\end{matrix}\right\} = \frac{1}{E[(b/a)^2-1]}\left[\frac{\{(1+\nu)[4(1-\nu)-\nu_c](b/a)^2 - \nu_c(1-2\nu)\}\mathcal{E}_c + 2(2-\nu)(1-\nu_c^2)(b/a)^2}{(1+\nu)[(1-2\nu)(b/a)^2+1]\mathcal{E}_c^2 + \{[3-\nu(1+4\nu_c)](b/a)^2 + (1+\nu)\}\mathcal{E}_c + 2(1-\nu_c^2)(b/a)^2}\right] p_i \tag{15}$$

The axial strain and displacement are

$$\left.\begin{matrix}\varepsilon_z|_{z=l} \\ \dfrac{w}{l}\Big|_{z=l}\end{matrix}\right\} = \frac{1}{E[(b/a)^2-1]}\left[\frac{(1+\nu)\{[1-4\nu_c(1-\nu)](b/a)^2 + (1-2\nu)\}\mathcal{E}_c + 2(1-2\nu)(1-\nu_c^2)(b/a)^2}{(1+\nu)[(1-2\nu)(b/a)^2+1]\mathcal{E}_c^2 + \{[3-\nu(1+4\nu_c)](b/a)^2 + (1+\nu)\}\mathcal{E}_c + 2(1-\nu_c^2)(b/a)^2}\right] p_i \tag{16}$$

The plane-strain solutions may be found directly by imposing $\varepsilon_z = 0$ in the previous analysis and finding the corresponding p_o by matching $u|_{r=b} = u_c|_{r=b}$. As an alternative approach, the plane-strain solution may be found from the plane-stress ($\sigma_z = 0$) solutions by making the following substitutions: $\nu/(1-\nu)$ in place of ν and $E/(1-\nu^2)$ in place of E. The plane-stress solution can be obtained directly or equivalently by setting $p' = p'' = 0$. Performing the above steps and considering no temperature loading ($\Delta T = 0$) the equations for plane strain are as follows:

The pressure between case and propellant at $r = b$ is:

$$\frac{p_o}{p_i} = \frac{2(1-\nu)}{[(1-2\nu)(b/a)^2 + 1] + \dfrac{2(1-\nu_c^2)}{(1+\nu)\mathcal{E}_c}\left(\dfrac{b^2}{a^2}\right)} \qquad (17)$$

10 indicates the variation of Poisson's ratio υ as defined in the preceding elastic analysis, with uniaxial tensile straining of a specimen. Incompressibility (no change in volume) is indicated by the upper curve. The lower curve represents an estimate of the increasing of volume which would be due mainly to vacuole formation about the oxidizer particles in a composite propellant.

In the strain test motors, hoop straining of a segment in the inner surface of the propellant ($r = a$) is not under the same loading conditions as that of a tensile specimen. The latter is not experiencing any sideways (normal) stresses whereas the actual stressing of the test motor segment does feel pressure in both normal directions (r and z) in addition to the hoop tension θ. This is analogous to having a hydrostatic pressure squeezing a tensile specimen from the sides while it is being pulled

The stress on the inside of the propellant is

$$\sigma_\theta|_{r=a} = \frac{1}{(b/a)^2 - 1}\left\{\frac{[(b/a)^2-1][(1-2\nu)(b/a)^2-1] + [(b/a)^2+1]\left[\dfrac{2(1-\nu_c^2)}{(1-\nu)\mathcal{E}_c}\right]\left(\dfrac{b^2}{a^2}\right)}{[(1-2\nu)(b/a)^2+1] + \dfrac{2(1-\nu_c^2)}{(1+\nu)\mathcal{E}_c}\left(\dfrac{b^2}{a^2}\right)}\right\} p_i \qquad (18)$$

The strain and displacement on the inner radius are

$$\left.\begin{matrix}\varepsilon_\theta|_{r=a} \\ \dfrac{u}{a}\Big|_{r=a}\end{matrix}\right\} = \frac{(1+\nu)}{E[(b/a)^2-1]}\left\{\frac{(1-2\nu)[(b/a)^2-1]^2 + \dfrac{2(1-\nu_c^2)}{(1+\nu)\mathcal{E}_c}\left(\dfrac{b^2}{a^2}\right)[(b/a)^2+(1-2\nu)]}{[(1-2\nu)(b/a)^2+1] + \dfrac{2(1-\nu_c^2)}{(1+\nu)\mathcal{E}_c}\left(\dfrac{b^2}{a^2}\right)}\right\} p_i \qquad (19)$$

The strain and displacement on the outer radius are

$$\left.\begin{matrix}\varepsilon_\theta|_{r=b} \\ \dfrac{u}{b}\Big|_{r=b}\end{matrix}\right\} = \frac{1}{E[(b/a)^2-1]}\left\{\frac{\dfrac{4(1-\nu)(1-\nu_c^2)}{\mathcal{E}_c}\left(\dfrac{b^2}{a^2}\right)}{[(1-2\nu)(b/a)^2+1] + \dfrac{2(1-\nu_c^2)}{(1+\nu)\mathcal{E}_c}\left(\dfrac{b^2}{a^2}\right)}\right\} p_i \qquad (20)$$

d. Variable Poisson's ratio. Poisson's ratio varies markedly with strain and is significantly dependent upon the type of loading and the resin-to-oxidizer bond. Figure

along its axis. This results in less of a voiding tendency and tends to cause υ to approach the incompressibility situation more closely.

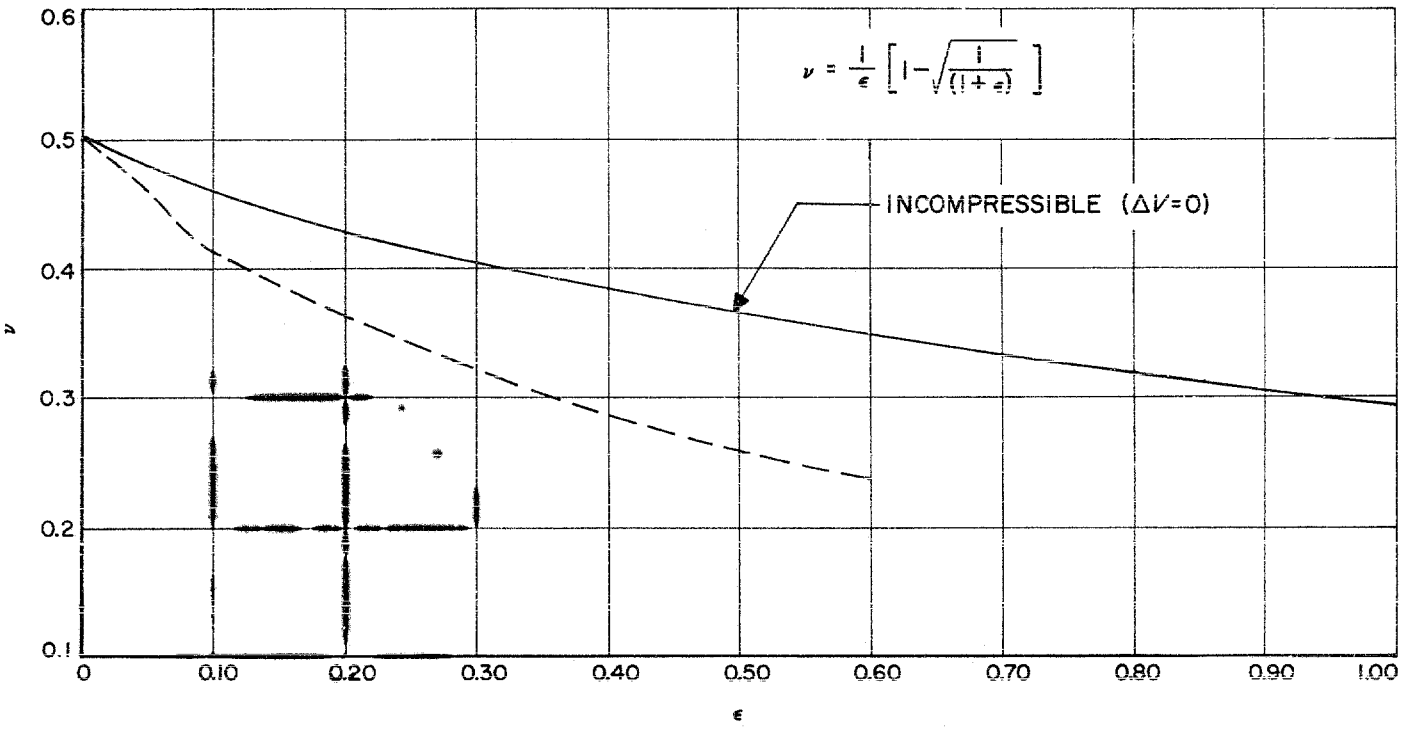

Figure 10. Poisson's ratio vs strain

2. Test Description and Results

The test motor (Fig 11) consists of a 7075-T6 aluminum chamber with a wall thickness of 0.040 inch in the center or test section of the case. The ends are tapered and threaded to accommodate a heavy end cap. Radial expansion of the case is thus confined to the center section at the test pressures which will be used. The inside diameter of the chamber is 2.646 inches and the web thickness is adjusted by the use of suitable mandrels from 1.000 to 0.265 inch in diameter to give $(b/a)^2$ ratios from 7 to 100.

A probe has been designed to monitor the radial displacement in the center of the test specimen. It consists of a steel ball ⅛ inch in diameter soldered to an 8-inch lever arm. On the other side of the pivot, the lever arm is attached to the core of a linear variable differential transformer, and the output of the transformer has been calibrated to monitor the radial displacement. The probe is held against the grain during pressurization by a small spring which exerts a 2-gram force.

Figure 12 is a schematic diagram of the strain-test-motor pressurization system which has been assembled and is now being checked out. Nitrogen at high pressure (about 500 psi) flows through an orifice into an accumulator whose void volume is preadjusted. The orifice and free volume predetermine the rate of pressure rise which is then amplified by an intensifier. Mineral oil is used downstream of the intensifier to pressurize the test motor at a rate which can be preset in the range from about 5 psi per second to about 50 psi per second. Calibration of the test equipment has been completed and the results have shown that the pressurization rate is linear over both the pressure range and rate range of interest. Provisions for recycling and remote operation have been included in the design.

A number of working charts have been prepared to facilitate the solution of the elastic equations. In Figure 13 the variables case pressure, inner stress, inner strain, and outer strain, are plotted against $(b/a)^2$ for different values of Poisson's ratio, all with an assumed propellant modulus of 10^3 psi. In Figure 14 the same variables are plotted against Poisson's ratio for different values of $(b/a)^2$, with the same assumed propellant modulus of 10^3 psi. Similar plots are available with assumed propellant moduli of 10^2 and 10^4 psi. Figure 13c illustrates graphically the extent to which a very small change in Poisson's ratio in the vicinity of $v = 0.5$ will affect the determination of inner strain. Discussion of reduction techniques and an evaluation of the validity of this analysis will be presented in succeeding reports.

The equipment has been designed to permit the study of grain behavior under thermal loading. This work will be undertaken upon completion of the pressurization phase of the program.

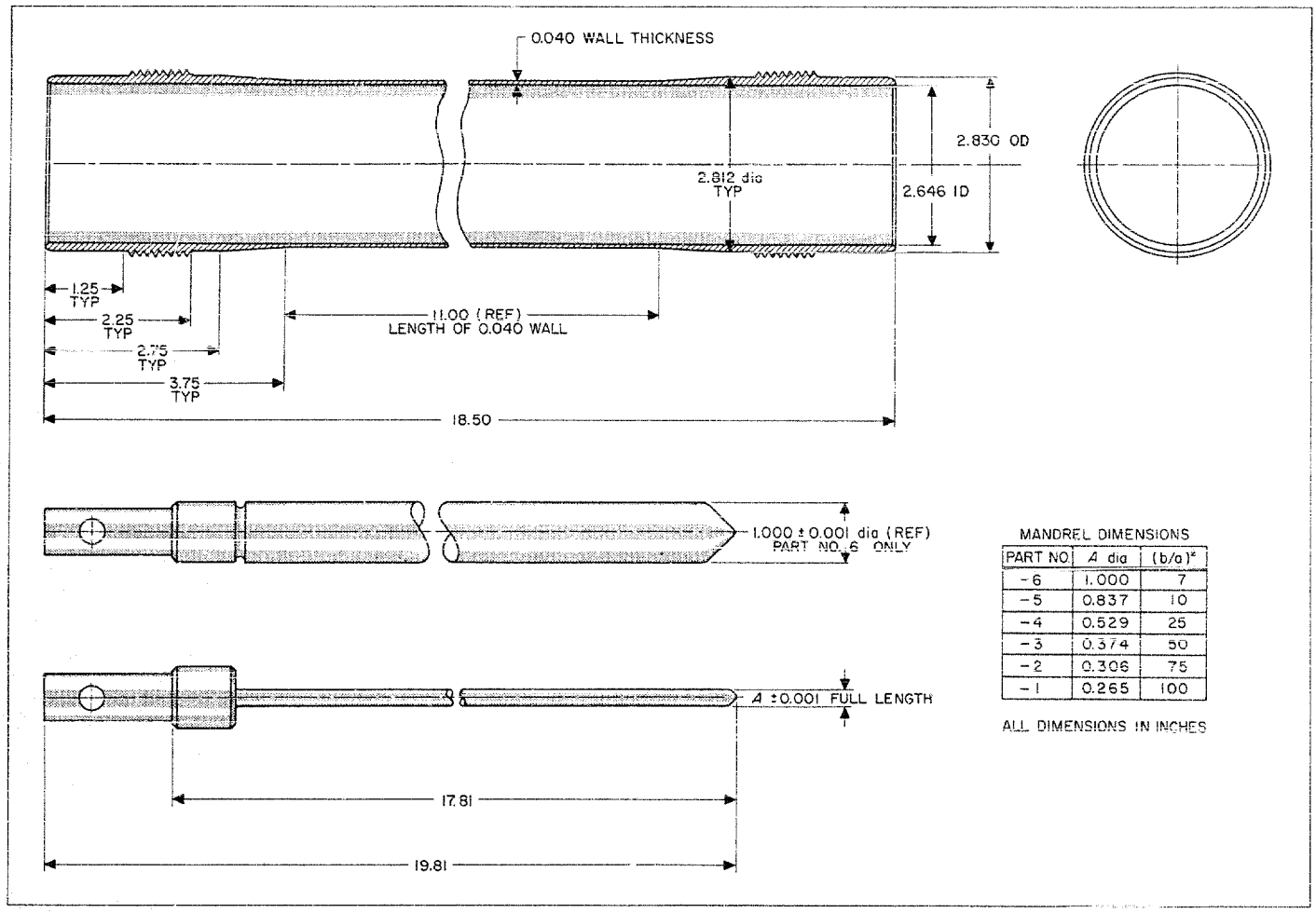

Figure 11. Strain-test motor case and mandrels

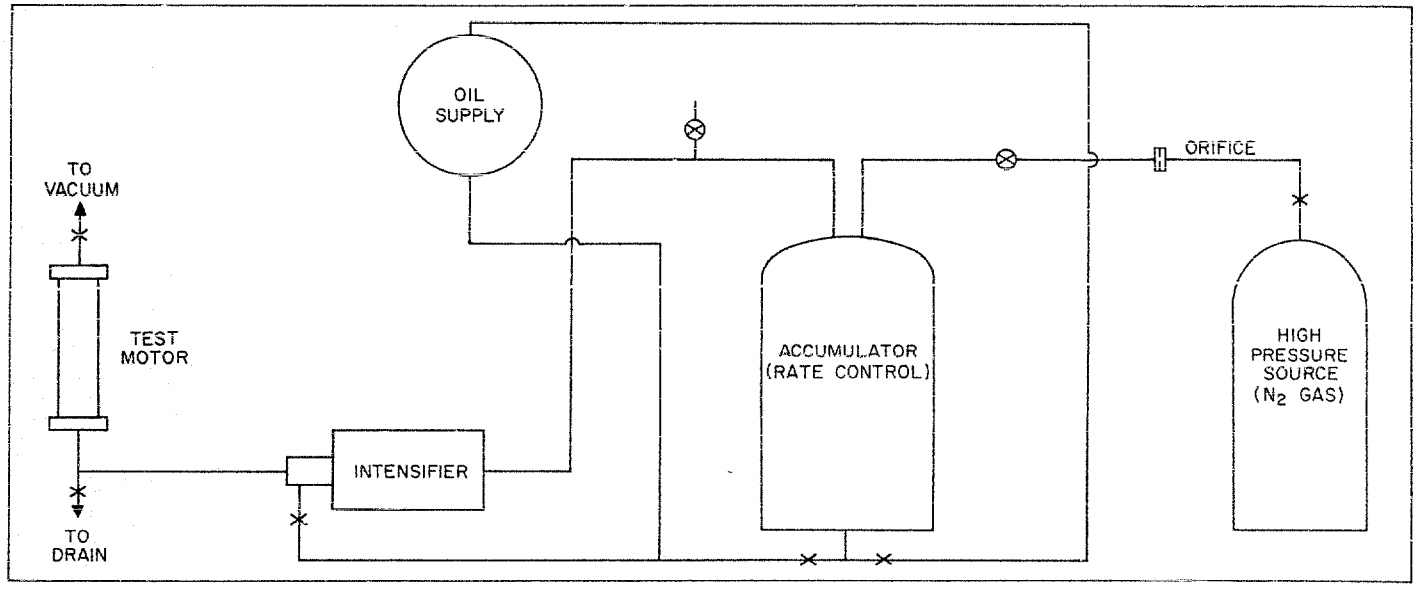

Figure 12. Strain-test motor-pressurization system

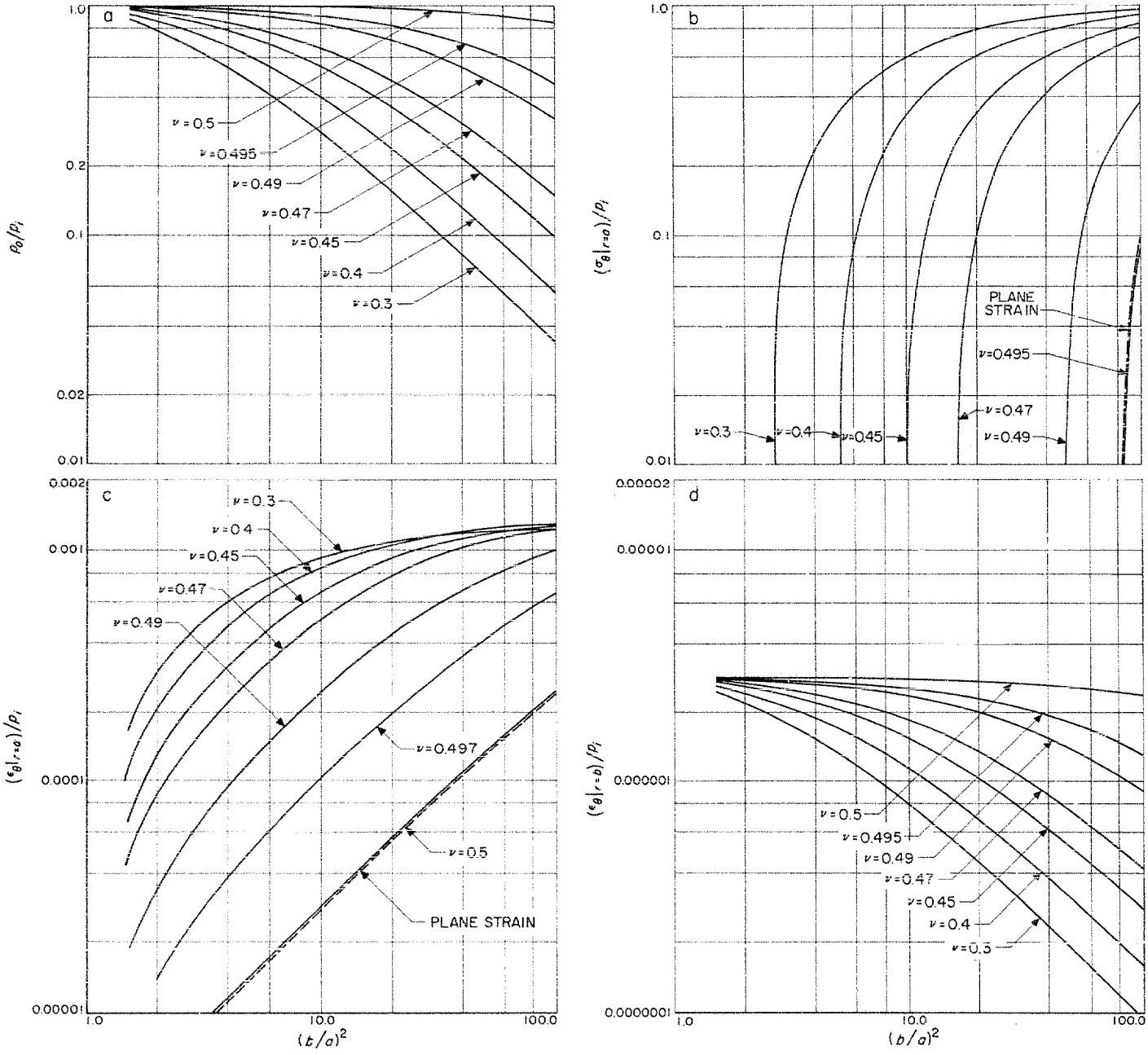

Figure 13. Dependence of elastic parameters on web dimensions for various Poisson ratios, propellant modulus = 10^3 psi

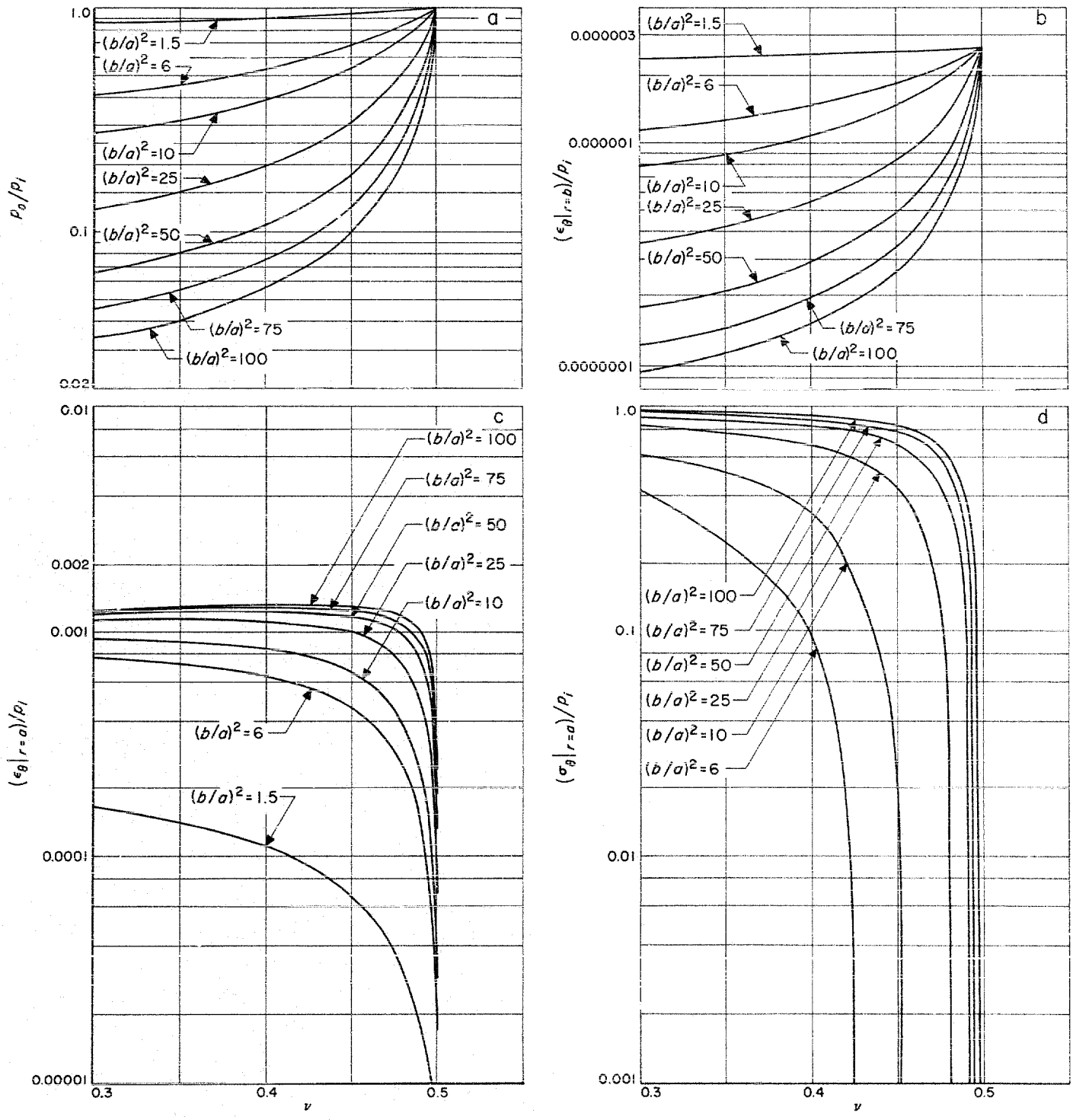

Figure 14. Dependence of elastic parameters on Poisson's ratio for various web dimensions, propellant modulus = 10^3 psi

III. BIBLIOGRAPHY

A. Radiography

A HIGH POWERED FINE FOCUS TUBE FOR THE FLUOROSCOPIC INSPECTION OF CAST PROPELLANT
Polansky, D. and Criscuolo, E. L.
October 24, 1955
Naval Ordnance Lab, White Oak, Md.
NAVORD 4148, 6 pp (CONFIDENTIAL)

This report describes the use of a high-power fine-focus X-ray tube (developed by Machlett Labs) which is capable of a continuous rating of 4000 kvp × ma above 70 kvp. The energy range available is from 30 kvp to 140 kvp with a measured focal spot of 0.5 to 0.6 mm. A sensitivity of 1.4% was attained using this tube in the fluoroscopic inspection of 1.8KS-7800 and 5KS-4500 grains. (SPIA/A18, #18,580)

INSPECTION OF ROCKET MOTORS BY NEUTRONS AND GAMMA RAYS
Todd, F. C.
March 22, 1957
Southwest Research Institute, San Antonio, Texas
Summary Report, 76 pp (CONFIDENTIAL)

(SPIA/A18, #18,552)

TELEVISION FOR THE INSPECTION OF CAST PROPELLANT
Polansky, D., Criscuolo, E. L., and Dyer, C. H.
September 19, 1957
Naval Ordnance Lab, White Oak, Md.
NAVORD 5722, 10 pp (CONFIDENTIAL)

A closed-link television chain, with 1029 line scan and an image orthicon tube, has been evaluated for the inspection of cast propellant. Penetrameter sensitivity of 2% can be obtained at a thickness of 6 inches. Due to brightness limitations of the fluorescent screen, 10 inches of propellant is the limiting thickness that can be penetrated by 250 kvp radiation and still present 5% sensitivity. The use of energies up to 2000 kvp for the detection of large voids in propellant thicknesses of 20 inches is feasible. A 31-inch diameter inert rocket motor (Thiokol type propellant) was inspected. The propellant has a perforated center with a total wall thickness of about 24 inches. In addition, small samples of different thicknesses were used to obtain basic absorption data. The limit of propellant inspection using high energy was determined. Since the motor had a perforated center it was possible to place the end of the 2000 kvp tube inside the motor. The television camera was placed outside. Under these conditions a hole ½ inch in diameter by about 8 inches long was detected. When the X-ray tube was placed outside the motor and the beam directed

so that it had to penetrate the entire motor, only high density foreign material in the motor was detectable. The fluorescent screen which is a major component of the television chain was investigated as to its efficiency and optimization of manufacturing variables. The Radelin PFG (ZnS) screen has a peak efficiency at 45 kev. At higher voltages the efficiency decreases until at 200 kev it is only 15% of the peak efficiency. A study of the fabrication parameters of screens, such as phosphor thickness, particle size and phosphor-to-binder ratio resulted in limited screen improvements. (SPIA/A18, #18,550)

POLARIS POWER PLANT DEVELOPMENT
November 30, 1957
Aerojet-General Corp., Sacramento, Calif.
3520-01Q-1 August–October 1957 (Includes work in MR 3520-1M-1 and -2, August–September 1957, 173 pp) (CONFIDENTIAL)

The use of radiography has been proven feasible in the determination of separations of liner from propellant and liner from chamber and of changes in density within the grain. Voids and cracks can be detected with scintillation-counting equipment. The monitoring of relative locations of radioisotopes appears to be the most encouraging method of measuring deformation in a propellant grain during curing, thermal cycling, and pressurization. (SPIA/A18, #18,038)

TECHNICAL PROGRAM REVIEW 1957: CHAPTER 6: PROPELLANTS AND PROPULSION FOR MISSILES
January 1, 1958
Naval Ordnance Test Station, China Lake, Calif.
NOTS 1875, Chapter 6, 29 pp (CONFIDENTIAL)

Various new gauges were developed for examining the irregularities of propellant-grain surfaces, and radiographic inspection progressed to the point that very large grains can be examined accurately for fissures and voids. (SPIA/A18, #18,351)

A COMPARISON OF X-RAY AND ULTRASONIC METHODS OF INSPECTION, APPLIED TO THE 2-INCH ABC CORDITE ROCKET CHARGE
Cole, L. D. and Mendoza, A. M.
March 18, 1958
Explosives Research and Development Establishment, Great Britain
7/M/58, 6 pp (CONFIDENTIAL)

A trial has been carried out to determine the applicability of the ultrasonic method of inspection to the 2-inch ABC cordite rocket charge. Twenty production charges were examined ultrasonically, and the records were compared with the radiographs. The charges were re-X-rayed and, where necessary, re-examined ultrasonically. Finally most of the charges were sectioned, to determine the exact size and type of each flaw. Both inspection procedures detected all important flaws, but a few very small ones were missed by both methods. Details are given of a new spray washing system for removing bubbles from the surface of the charges, and of a jig for correct positioning of the charges for radiography. Techniques for both methods of inspection are described. An analysis is given of the correctness of X-ray inspection on a limited number of charges, and it is indicated that all charges were sentenced correctly. (SPIA/A18, #18,329)

QUARTERLY REPORT [SOLID PROPELLANT, ROCKET MOTOR, AND IGNITER DEVELOPMENT]
July 1958
Redstone Arsenal, Ordnance Missile Labs, Huntsville, Ala.
3M7N26, April–June, 1958, 65 pp (CONFIDENTIAL)

"Development of the Rapid X-ray Fluorescence Method for Quality-Control Analysis of Propellants." A project was initiated to develop a rapid X-ray fluorescence method for the semi-continuous or continuous direct analysis of uncured ammonium perchlorate/polysulfide propellants. A general solution method applicable to cured and uncured propellants is also being investigated. The direct analysis method consists of comparing characteristic-emission-line intensities from the surfaces of a standard and an unknown. The concentration of the particular constituent in an unknown is determined by simple proportionality. A single sample can be analyzed in 5 to 7 minutes; however, in practice, duplicate or triplicate analyses will be required to obtain sufficient analytical accuracy. (SPIA/A18, #18,415)

POLARIS POWER PLANT DEVELOPMENT
July 20, 1958
Aerojet-General Corp., Sacramento, Calif.

3520-01M-9, June 1958, 115 pp
(Also under Patent Secrecy Orders)
(CONFIDENTIAL)

Analysis of data from gamma-ray experiments with inert propellant samples instead of lucite samples was performed. At the source end, the smallest size void that can be detected with a probability of 0.90 or greater is ⅛ by ½ inch. At the detector end, the smallest size cylindrical void and saw-cut void that can be detected with a probability of 0.90 or greater is ⅛ by 1 and 0.06 inch by 48 inches, respectively. Dynamic tests (the propellant was moved, relative to the source and detector, during the test) were conducted at the Naval Ordnance Test Station to determine the minimum size of voids that could be detected in propellant with the radial readout detection system. The minimum detectable void depth was determined with the radial readout detection system. The minimum detectable void depth was determined as a function of rate-meter time constant, void width, scanning speed, detector collimation, and attenuation thickness, using a 1.1-curie cobalt 60 source. Under certain conditions, a void ¼ by ⅛ by 0.240 inch could be detected with 3-σ confidence. A comparison of results with 150-kev and 2-mev X-ray systems is given. (SPIA/A18, #18,343)

MINUTEMAN. MONTHLY TECHNICAL PROGRAM REPORT FOR AUGUST 1958

Taylor, R. G. and Cobb, E. L.
Thiokol Chemical Corp., Ogden, Utah
TPMO-15-58, 43 pp (CONFIDENTIAL)
AF 33(600)-36514

The Nuclear Systems Division of Budd Co. has completed a program to study and analyze non-destructive inspection methods for solid propellant charges. Five systems were evaluated in terms of cost, thickness limits, sensitivity, and speed of inspection. A summary of this evaluation is tabulated. It was concluded that gamma probing offers the best potential for development of an adequate automatic inspection system. (SPIA/A18, #18,454)

POLARIS POWER PLANT DEVELOPMENT

September 20, 1958
Aerojet-General Corp., Sacramento, Calif.
3520-01M-11, August 1958, 102 pp
(Also under Patent Secrecy Orders)
(CONFIDENTIAL)

A 1000-curie cobalt-60 radiographic source tested to determine its relative merit as compared with the 2-mev X-ray process has shown the two methods to be equally sensitive. (SPIA/A18, #18,512)

JANAF: SYMPOSIA ON SCALE AND NONDESTRUCTIVE TESTING

October 1958
Johns Hopkins University, Applied Physics Lab, Silver Spring, Md.
JANAF Solid Propellant Rocket Static Test Panel Meetings–SSNT, Papers (CONFIDENTIAL)

The following papers are given: scale testing of BDI, a cast double-base formulation; small scale testing; an analysis of 5-inch test motor firing in the T50 and T52E3 Jato programs; the prediction of static firing results of Jato M5 (*Nike-Ajax* boosters) from small-scale test data; comparisons of ballistic properties of scale model and full-size *Sergeant* motors; internal inspection of large solid propellant propulsion units by radiological methods; and non-destructive techniques for propellant evaluation: Part I—General description and application.

NONDESTRUCTIVE TESTING OF POLARIS MISSILE MOTORS

September 29, 1958
USNAD, Quality Evaluation Lab, Concord
QE/CO 58-25, 12 pp (CONFIDENTIAL)

This report describes the operational procedures and the evaluation of test results as obtained in the nondestructive examination of 1st and 2nd stage Polaris motors 1-PAL-2 and 2-PA-9 at NAD by use of a 2-mev X-ray unit, a 720 curie cobalt-60 gamma source, an ultrasonic scanner employing a Type UR Reflectoscope and a borescope. A discussion is also presented on the possible application of neutron radiography. (SPIA/A18, #18,553)

POLARIS POWER PLANT DEVELOPMENT

November 20, 1958
Aerojet-General Corp., Sacramento, Calif.
3520-01M-13, October 1958, 93 pp
(Also under Patent Secrecy Orders)
(CONFIDENTIAL)

Two portable gamma ray-scintillation detectors for testing motors for separations will be designed and fabricated. (SPIA/A18, #18,565)

REFRACTORY MATERIALS SUITABLE FOR USE IN GUIDED MISSILE PROPULSION SYSTEMS

Nicholson, K. C.
December 12, 1958
The Carborundum Co., Niagara Falls, N. Y.
Third Quarterly Report, September–November 1958
NOrd 18136-1, 28 pp (CONFIDENTIAL)

X-ray inspection data for some nozzle inserts showed porous areas which had not been detected by visual inspection alone. Subsequently, it was found that most of the voids could be eliminated by modification of the siliconizing technique. (SPIA/A18, #18,619)

NONDESTRUCTIVE TESTING OF SOLID PROPELLANTS: AN ANNOTATED BIBLIOGRAPHY

Cole, J. W.
December 12, 1958
Solid Propellant Information Agency, Silver Spring, Md.
SPIA/B5, NOrd 7386 (CONFIDENTIAL)

NONDESTRUCTIVE TESTING OF SOLID PROPELLANT: SUPPLEMENT A TO AN ANNOTATED BIBLIOGRAPHY

Cole, J. W.
March 4, 1959
Johns Hopkins University, Applied Physics Lab, Silver Spring, Md.
SPIA/B5, NOrd 7386 (CONFIDENTIAL)

POLARIS POWER PLANT DEVELOPMENT

December 20, 1958
Aerojet-General Corp., Sacramento, Calif.
3520-01M-14, November 1958, 90 pp
(Also under Patent Secrecy Orders)
(CONFIDENTIAL)

"Development of Inspection Techniques for Propellant Grains" (Appendix D). A tabular summation of inspection techniques for flaw detection was given in Report No. L0162-01-Q1, June 1958. Present work consists of refinements made in the use of scintillation crystal detectors with a source of cobalt-60 and the interpretation of recorded data. The physical setup and statistical computations are described for the calculation of scattering effect, absorption coefficients, confidence levels and sensitivity in a system containing introduced voids of known geometry. Computers for data reduction were also evaluated. (SPIA/A18, #18,593)

POLARIS POWER PLANT DEVELOPMENT

January 20, 1959
Aerojet-General Corp., Sacramento, Calif.
3520-01M-15, December 1958, 75 pp
(Also under Patent Secrecy Orders)
(CONFIDENTIAL)

"Development of Inspection Techniques for Propellant Grains" (Appendix C). This section covers tests and studies performed during October 1958 utilizing a cobalt-60 source, scintillation counters and a data reduction computer (IBM-650) for the detection and interpretation of motor flaws. The entire surface of the motor is scanned by a set of counters that sweep the surface in a number (usually 51) of discrete vertical locations. (SPIA/A18, #18,594)

POLARIS POWER PLANT DEVELOPMENT

Kirchner, W. R.
February 20, 1959
Aerojet-General Corp., Sacramento, Calif.
3520-01M-16, January 1959, 87 pp
(Also under Patent Secrecy Orders)
(CONFIDENTIAL)

"Development of Inspection Techniques for Propellant Grains" (Appendix E). A description is given of the physical layout of the Sacramento test facility, radiation source handling, scintillation detectors and associated electronic components. A series of experiments was performed to determine the sensitivity of the gamma-ray scintillation inspection system to separations between the liner and the chamber and/or the grain. The separations were obtained by inserting shims of known thickness in the desired location and bolting together the test pieces. The correct position of the sample with respect to the source and detector collimator was established with a straight edge, and the test piece was clamped firmly to the bench. The liner used for these tests was a curved piece of lucite (density: 1.2 gm/cc), and the grain was live propellant (density: 1.7 gm/cc). It was not possible to determine the exact sensitivity of the skin-scan system from the test results because of apparent deviations in alignment of the sample. However, lower limits were established for

the sensitivity of each width collimator, using 20 curies of cobalt-60, 9 seconds of inspection time, and 30.5-inch distance between the source and the detector crystal. Ten tests were performed to determine the linear attenuation coefficient of active propellant for cobalt-60 photons.

It is extremely difficult to arrive at specific conclusions from the test data concerning the effect of the various parameters because of the unresolved effect of the scattering. However, this can be stated: (1) the linear attenuation of photons through active propellant is 0.24/inch, (2) ½ inch of Mallory filter reduced the counts by a factor of 2.5, and (3) the effect of source collimation on the count rate is negligible. Extrapolation of experimental data obtained by radial-readout and flipping finger systems showed that a void ¾ inch deep by 1 inch high by 1/32 inch wide can be detected with better than 95% confidence.

Results of tests performed to determine the feasibility of reducing the detector high voltage to obtain useful inspection data from detectors that otherwise would be recording more than 10^6 counts indicate that the effect of a voltage change is about the same as is observed by a change in source strength. Apparently the effect of voltage change on photon energy is negligible in the voltage regions investigated. The effect of voltage drift on void detectability was also investigated. The results of the drift tests show that, if the voltage can be held to about ±0.2 volt, the effect on the detectability of voids will be negligible.

"Chamber-to-Liner Bond Evaluation" (Appendix F). The quality of the steel-to-liner interface can be determined as a meter reading by an ultrasonic echo device. The instrument chosen to provide an ultrasonic echo pattern is a Sperry Products, Inc., echo-thickness gage which has been modified to include echo-processing circuits. The function of the various electronic components of the system is detailed. (SPIA/A19, #19,067)

NONDESTRUCTIVE TECHNIQUES FOR THE DETERMINATION OF PHYSICAL INTEGRITY OF ROCKET MOTORS

August 1959
Johns Hopkins University, Applied Physics Lab, Silver Spring, Md.
Meetings, NOrd-7386 (CONFIDENTIAL)

Ten papers on nondestructive techniques for testing solid propellants are included in this report. Some of the methods are, X-ray, cobalt-60, gammagraph, betatron radiography, ultrasonic techniques, infrared, fluoroscopy and fluorography, gamma scintillation, and ion chamber inspection.

THE EFFECT OF GAMMA RADIATION FROM COBALT-60 ON THE MECHANICAL PROPERTIES OF AHH AND ARP DOUBLE-BASE SOLID PROPELLANTS (U)

Marciniak, W. J. and Phillips, T. D.
July 1, 1959
U.S. Naval Propellant Plant, Indian Head, Md.
TMR-159 (CONFIDENTIAL)

The irradiation of AHH and ARP resulted in considerable damage to both propellants. At the maximum dosage (38.2 megaroentgens), the mechanical properties were drastically reduced. The resin coating used to retard the swelling of casting powder granules during processing does not alter the effect of irradiation on the cast grain.

THE DEVELOPMENT OF NON-DESTRUCTIVE TEST METHODS FOR THE INSPECTION OF SOLID PROPELLANT (U)

Polansky, D., Criscuolo, E. L., et al
October 5, 1959
Naval Ordnance Laboratory, White Oak, Md.
NAVORD-R-6716 (CONFIDENTIAL)

This report reviews the work conducted during the past 5 years in the development of X-ray methods for the inspection of solid propellant. Details on fluoroscopy, fluorography and television methods are given, in addition to the sensitivity limits as applied to various propellant thicknesses.

NONDESTRUCTIVE EVALUATION OF SUBROC PROPULSION UNITS (U)

Bacher, A. A.
November 18, 1959
U. S. Naval Propellant Plant, Indian Head, Md.
TMR-175 (CONFIDENTIAL)

This report is concerned with the static test performance of two grains and the relationship between the performance and the results of nondestructive inspection of these propellant grains.

POLARIS POWER PLANT DEVELOPMENT (U)

January 20, 1960
Aerojet-General Corp., Azusa, Calif.
R-3520-01M-27 (CONFIDENTIAL)

Appendix D: contains nondestructive testing information and compares firing data.

ADVANCEMENT OF SOLID PROPELLANT ROCKETRY: Quarterly Progress Report of Army Supporting Research
February 8, 1960
Thiokol Chemical Corp., Redstone Division, Huntsville, Ala.
R 1-60 (CONFIDENTIAL)

Continuation of exploratory research for determination of the feasibility of a method for X-ray detection of flaws in solid propellant rocket motors and component parts by use of scintillating crystals as detectors has produced encouraging results. Tests indicate that X-rays from a 120 kv source are converted into visible light in the first few hundredths of an inch of thickness of high electron density in iodide scintillating crystals. Thicker crystals attenuate and diffuse the light.

NON-DESTRUCTIVE TESTING OF LARGE SOLID PROPELLANT CASE-BORDED ROCKET MOTORS
Cusick, J. H.
Non-destructive Testing, Vol 18, No. 3, May–June 1960

B. Ultrasonics

ULTRASONIC TESTING BY THE RESONANCE METHOD
ASTM Designation: E 113-55T

This recommended practice covers a procedure for measuring the thickness of materials from one side by the ultrasonic resonance method. Also included are recommendations for using this method for locating certain types of discontinuities in materials.

ULTRASONIC TESTING BY THE REFLECTION METHOD, USING PULSED LONGITUDINAL WAVES INDUCED BY DIRECT CONTACT
ASTM Designation: E 114-55T

This recommended practice covers a procedure for ultrasonically testing for inhomogeneity in sonic conducting materials by the reflection method, using pulsed longitudinal waves introduced by direct contact of the searching unit with the material being tested. Recommendations are also given for measuring thickness dimensions from a testing surface.

TEMPERATURE DEPENDENCE OF ULTRASONIC VELOCITY IN PLASTICS
Subrahmanyam, S. V.
Journal of Chemical Physics, Vol 22, pp 1562–1563, September 1954

The composite piezoelectric oscillator method has been employed to study the temperature dependence of the velocity of ultrasonic waves in Perspex and polystyrene plastics. While confirming a previously reported transition in Perspex at 60°C the results show the existence of a transition in polystyrene also at 70°C for the first time. (P.A., 1954, #10,899)

THE ULTRASONIC INSPECTION OF PROPELLANTS: PART 4: ELECTRONIC CIRCUITRY FOR A TWO-CHANNEL FLAW DETECTOR
Eldridge, D. A. G. and Short, A. D.
December 1956
Explosives Research and Development Establishment, Great Britian
TM 16/M/56, 7 pp (CONFIDENTIAL)

Improvements suggested in Part 3 of the series have been incorporated in new miniaturized two-channel equipment. The added channel makes it possible for cruciform charges to be totally inspected during one scan; alternatively the equipment may be used to provide independent inspection of two separate charges. Description of circuit changes together with new circuit diagrams gives a complete record of the design of this latest equipment. (SPIA/A17, #17,019)

AN ULTRASONIC METHOD OF DETECTING LACK OF ADHESION BETWEEN CASE-BONDED PLASTIC PROPELLANT AND THE TUBE WALL IN ROCKET MOTORS
Lister, R.
November 1957
Royal Aircraft Establishment, Westcott, Great Britian
TN R.P.D. 156, 7 pp (CONFIDENTIAL)

In a rocket motor containing a case-bonded propellant charge, the motor tube serves the dual purpose of supporting the propellant and forming an inhibited surface. The inspection of a rocket motor tube containing case-bonded propellant should therefore determine the adherence of the propellant to the case. An ultrasonic method has been developed, using only external devices, which gives clear and precise indications of defective adhesion. The method is based on use of transverse ultrasonic waves generated by transverse probes having preferably a 10-degree angle of transmission in steel. Care is taken to select a frequency which gives a wavelength less than the thickness of metal. Defects down to very small sizes (0.5 by 0.0015 in.) can be detected, and by varying the distance between the probes this distance can be detected and correlated to a definite size of defect. The desired minimum size of defect can be selected and nothing smaller than this need be revealed. The method is amenable to automatic methods of operation recording. Exploratory work shows promise of being able to apply the technique to the inspection of bonds between metal and plastics of the resin/asbestos type and also between metal and glass fibers. (SPIA/A18, #18,097)

THE E.R.D.E. ULTRASONIC FLAW DETECTOR MARK III: DESIGN AND DEVELOPMENT OF A HIGHLY SENSITIVE INSTRUMENT FOR THE INSPECTION OF VERY THICK THERMOPLASTIC MATERIALS

Eldridge, D. A. G. and Short, A. D.
February 1958
Explosives Research and Development Establishment, Great Britian
TM 1/M/58, 18 pp (CONFIDENTIAL)

This memorandum describes the development of a highly sensitive two-channel ultrasonic flaw detector devoloped from the E.R.D.E. Ultrasonic Flaw Detector Mark II. A number of the Mark II models are being used to detect defects in some of the smaller thermoplastic samples i.e., up to eight-in. external diameter. Extra sensitivity is gained in the Mark III equipment by increasing the power of the ultrasonic wave transmitted through the test sample and by increasing the gain of the amplifier to which the signal from the receiver transducer is applied. It is now possible to detect flaws in samples of up to twenty-inch thickness, but the smallest detectable flaw size in this thickness of material has not been established. The high-gain negative feedback amplifier used in this model could, by one complete chassis change, be incorporated in an existing Mark II model. (SPIA/A18, #18,164)

THE ACOUSTIC PROPERTIES OF SOLID PROPELLANTS AT ULTRASONIC FREQUENCIES

Cole, L. D., Seaman, R. E., and Vernon, J. H. C.
Explosives Research and Development Establishment, Great Britian
2/R/58, 14 pp (CONFIDENTIAL)

A knowledge of the way in which sound waves travel through solid and liquid media, and of how they are reflected, refracted, and absorbed, is important for the setting up of an ultrasonic inspection system. Measurements and calculations of sound velocities, refractive indices and critical angles for materials of importance in flaw detection systems are described. The application of such data to the setting up of inspection systems, and the choice of immersion media for double-base solid propellant charges of complex cross-section, such as Mayfly and Gosling, are demonstrated. The energy losses at cordite/water interfaces are evaluated. Measurements are described of the attenuation of sound in solid propellants, and in the liquid in which they are immersed. An evaluation of the transducer and electrical losses completes the study of the various ways in which the energy may be dissipated, and enables estimates to be made of the total penetrative power of the E.R.D.E. Ultrasonic Flaw Detector for any solid propellant charge of the double-base type. (SPIA/A18, #18,330)

POLARIS POWER PLANT DEVELOPMENT

October 20, 1958
Aerojet-General Corp., Sacramento, Calif.
3520-01M-12, September 1958, 120 pp
(Also under Patent Secrecy Orders)
(CONFIDENTIAL)

An instrument that utilizes various electronic circuits is under development to give a direct meter reading showing the quality of bond at the steel-to-liner and at liner-to-propellant interfaces. Insulation on the closures of *Polaris* motors in process has been found to be unbounded. Ultrasonic bond inspection has been initiated as a process-control tool to discover the lack of bonding. The insulation was cut open and repaired, and subsequent ultrasonic inspection showed a good bond. The minimum temperatures at which ANP-2639AF cannot be shock initiated to explosion are −60°F (for an 8.5-gm tetryl booster) and −20°F (for a 46-gm tetryl booster). The corresponding temperatures for ANP-2655AF are −40°F and −20°F. (SPIA/A18, #18,526)

C. Infrared

QUARTERLY PROGRESS REPORT
[COMPOSITE PROPELLANT RESEARCH AND DEVELOPMENT]
Thiokol Chemical Corp., Redstone Division, Huntsville, Ala.
25-58(C-C-58-2749), January–March, 1958, 42 pp
(CONFIDENTIAL)
(DA-01-021-ORD-5314)

"Use of Infrared Radiation in Bond Evaluation." One of the most difficult conditions to determine during inspection of case-bonded internal-burning solid-propellant motors is bond failure between the propellant and liner or between the liner and the motor case. On the hypothesis that the heat transfer coefficient is less across an unbonded metal-to-propellant interface than across a well bonded interface, a decision was made to evaluate an infrared method of motor inspection. A Barnes Far-Infrared Camera (described in this report) was obtained, and two XM30 28-inch *Nike B* test motors and two TX19 Recruit motors were examined with this apparatus. One XM30 and one TX19 motor were conditioned at 0°F for 5 days. The remaining XM30 and TX19 motors were conditioned for 5 days at 170°F. The XM engine conditioned 170°F was known to have large areas in which the propellant and liner had pulled away from the motor case. A photograph of this motor is shown. Dark areas near the top and bottom center of the photograph represented areas of temperature gradients; they were found in the general location of known voids. It was concluded that the inspection of case-bonded internal-burning solid propellant motors by infrared radiation was feasible, although limited by the equipment available. The equipment employed was capable of discerning temperature differences of 0.2°C; however, the signal to noise ratio at this level of amplification was quite low. The Barnes Engineering Company is undertaking further developmental work in an endeavor to produce a scanning device that will operate on thermal gradients only. (SPIA/A18, #18,493)

QUARTERLY PROGRESS REPORT ON INTERIOR BALLISTICS (U)
Brandon, W. W. and DeMore, J. E., et al
August 31, 1959
Rohm & Haas Co.
Redstone Arsenal Research Division, Huntsville, Ala.
R-P-59-1 (CONFIDENTIAL)

A mathematical analysis was made of the possibility of using infrared photography for the detection of case bond failures.

D. Miscellaneous

SYMPOSIUM ON NON-DESTRUCTIVE TESTING: PRESENTED AT THE FIFTY-FIFTH ANNUAL MEETING
Fiftieth Anniversary Meeting, American Society for Testing Materials, New York, N.Y., June 26, 1952; Philadelphia, Pa., 1953

RÉSUMÉS OF FACILITIES, METHODS, AND WORK AT PARTICIPATING ORGANIZATIONS
Solid Propellant Information Agency, Silver Spring, Md.
JANAF Solid Propellant Surveillance Panel
SPSP/1 (CONFIDENTIAL)
NOrd-7386

PROCEEDINGS OF THE FIRST MEETING OF THE JOINT ARMY-NAVY-AIR FORCE SOLID PROPELLANT SURVEILLANCE PANEL
April 16–18, 1957
Solid Propellant Information Agency, Silver Spring, Md.
SPSP/2 (CONFIDENTIAL)
NOrd-7386

The methods and facilities employed at the various laboratories and agencies of the Navy, and the programs used by Army and Air Force are described. Problems in accelerated aging tests are considered and the use of "model" motors in surveillance programs described.

BULLETIN OF THE SECOND MEETING OF THE JOINT ARMY-NAVY-AIR FORCE SOLID PROPELLANT SURVEILLANCE PANEL
November 14, 15, 1957
Solid Propellant Information Agency, Silver Spring, Md.

SPSP/3 (CONFIDENTIAL)
NOrd-7386

The two sections concern storage degradation of solid propellants and screening criteria for new propellant formulations. The former includes articles on thiokol polysulfide engines; creep failure in the *Sergeant* motor; surveillance on the M35 (T205) rocket motor; stability of small arms propellant; elevated temperature storage; and limitations of double base propellants. The latter section includes papers on autoignition and thermal decomposition; the role of impact and gap testing; screening through stability, physical and ballistic testing; nitrocellulose stability; methods for studying stability and chemical structure of composite propellants and their polymeric binders; and a plan of attack in development of new propellants.

JANAF SOLID PROPELLANT SURVEILLANCE PANEL: BULLETIN OF THE SECOND MEETING
November 1957
Solid Propellant Information Agency, Silver Spring, Md.
Meetings-2-SPSP Bulletin, (Addendum)
SPSP/4 (CONFIDENTIAL)

Papers from the symposium on storage degradation of solid propellants and rockets and from the symposium on screening criteria for new propellant formulations are presented.

THE PROPAGATION OF STRESS WAVES IN VISCOELASTIC SOLIDS
Kolsky, H.
Applied Mechanics Reviews, Vol 11, No. 9, pp 465–468, 1958

NONDESTRUCTIVE TESTS AND QUALITY CONTROL
Frohmberg, R. P.
Astronautics, Vol 3, No. 7, pp 32–33, July 1958

JANAF SOLID PROPELLANT SURVEILLANCE PANEL: BULLETIN OF THE THIRD MEETING
October 1958
Solid Propellant Information Agency, Silver Spring, Md.
Meetings-3-SPSP, Bulletin
SPSP/5 (CONFIDENTIAL)

The following papers are included: propellant behavior at low temperatures; the storage stability of some ammonium perchlorate/polyurethane propellants; surveillance of the torpedo booster motor Mark 1 Mod 0 of the rocket-thrown torpedo; non-destructive techniques for propellant evaluation: Part II: prediction of aging characteristics; and a comparison of the surveillance characteristics of the *Sergeant* motor with laboratory and scale-motor tests.

JANAF SOLID PROPELLANT SURVEILLANCE PANEL: BULLETIN OF THE THIRD MEETING
October 1958
Solid Propellant Information Agency, Silver Spring, Md.
Meetings-3-SPSP, Bulletin (Addendum)
SPSP/6 (CONFIDENTIAL)

The three papers presented at the session on "Propellant Evaluation and Prediction of Aging Characteristics of Large Motors" are given and six papers related to solid propellant test methods are presented.

SYMPOSIUM ON SCALE AND NONDESTRUCTIVE TESTING
January 1960
Solid Propellant Information Agency, Silver Spring, Md.
JANAF Solid Propellant Rocket, Static Test Panel Meetings—SSNT (Addendum)
SP S-NDT/1A, October 1958 (CONFIDENTIAL)

A STUDY REPORT ON THE PRESENT STATUS OF NONDESTRUCTIVE TESTING AS APPLIED TO SOLID PROPELLANTS
Tenney, G. H.
October 15, 1958
Los Alamos Scientific Laboratory, N.M.

GRAPHICAL COMPILATION OF RADIATION EFFECTS ON MECHANICAL PROPERTIES OF SOLIDS
November, 1958
Aerojet-General Corp., Azusa, Calif.
WADC-TN-58-335,
R 1519, AF 33(616)5552, (Available AEC)

A PHOTOELASTIC APPROACH TO TRANSIENT STRESS PROBLEMS EMPLOYING LOW MODULUS MATERIALS
Dally, J. W., Riley, W. F., et al
December 1958
Illinois Institute of Technology, Chicago
Armour Research Foundation Report
AF 18(603)-144

NON-DESTRUCTIVE TESTING
Hinsley, J. F.
Macdonald & Evans, London, 1959
(With a foreword by Edwin Gregory)

NONDESTRUCTIVE TESTING HANDBOOK
Vols I and II
McMaster, R. C., Editor
Ronald Press Co., New York, 1959

EVALUATION OF SOLID PROPELLANT PROPERTIES: PART I: A SURVEY OF CURRENT METHODS
Warren, F. A., Anderson, E. L., and Ku, P. M.
January 31, 1959
Southwest Research Institute, San Antonio, Texas

EVALUATION OF SOLID PROPELLANT PROPERTIES: PART II: A CRITICAL EXAMINATION OF CURRENT METHODS
Warren, F. A.
January 31, 1959
Southwest Research Institute, San Antonio, Texas

RESEARCH STUDY TO ADVANCE THE STATE-OF-THE-ART OF SOLID PROPELLANT GRAIN DESIGN
Thiokol Chemical Corp., Elkton, Md.
QPR-1 (CONFIDENTIAL)
AF 33(616)-6530

The initial phase of the program was concerned with determining the effects of grain design on rocket engine capabilities, improving the methods and techniques of grain design and studying the effects of propellant physical properties on grain design. A literature search was made and a bibliography of more promising sources of information compiled.

AGING PROPERTIES OF SOLID PROPELLANTS FOR ROCKET MOTOR
June 30, 1957–September 30, 1959
Christensen, L. D. and White, B. B.
Stanford Research Institute, Menlo Park, Calif.
R 75 (CONFIDENTIAL), AF 33(038)-28634

Paralleling the propellant evaluation effort has been continued pursuit of new techniques for detecting and measuring changes in propellant properties, particularly techniques sensitive to the changes in propellant properties with age. The ultimate goal has been to determine the feasibility of, and to develop, nondestructive aging detection devices for use by field personnel. In general, the most effective methods of following propellant aging were found to be: (1) tensile creep; (2) Young's modulus at low temperature; (3) shear strength and, to a lesser degree, (4) microscopic examination of microtomed propellant sections. Shear strength is useful for polysulfide propellants, but does not work well with polyurethanes. Two nondestructive techniques, the STAG-meter and EPR spectroscopy, have promise, but are not sufficiently developed at present.

INVESTIGATION OF CREEP BEHAVIOR OF PROPELLANT MATERIAL
George, D. A.
September 4, 1959
Commerce Dept., National Bureau of Standards, Washington, D .C.
PR-19, R-6571, TU 2-2Q

FRACTURE MECHANICS OF SOLID PROPELLANTS (U)
Jones, J. W.
October 1959
DuPont de Nemours, E. I., & Co., Inc.
Explosives Dept., Wilmington, Delaware
Elas-A-15 (CONFIDENTIAL)
NOord-18138

Triaxial tensile tests were made at a strain rate of 10%/min of ANP-2639AF propellant. The Model 2 high rate test apparatus was calibrated and a limited number of high rate tensile tests of the same propellant were made. Design details and operating data for the tester are given.

JANAF SOLID PROPELLANT SURVEILLANCE PANEL: BULLETIN OF THE FOURTH MEETING

December 10, 11, 1959
Solid Propellant Information Agency,
Silver Spring, Md.
Meetings-4-SPSP, Bulletin
SPSP/7 (CONFIDENTIAL)

RESEARCH STUDY TO ADVANCE THE STATE-OF-THE-ART OF SOLID PROPELLANT GRAIN DESIGN

December 30, 1959
Thiokol Chemical Corp., Elkton, Md.
QPR-2, AF 33(616)-6530

This report includes a literature survey on the structural analysis of solid propellant grains. Some of the configurations that showed promise are being analyzed.

FRACTURE MECHANICS OF SOLID PROPELLANTS (U)

Jones, J. W., and Sagers, D. L.
January 1960
DuPont de Nemours, E. I., & Co., Inc.
Explosives Dept., Wilmington, Del.
ELab-A-18 (CONFIDENTIAL)
NOrd-18138

The uniaxial tensile properties of ANP-2655 and ANP-2639 propellants, measured at temperatures between −6 and 103°F at strain rates between 0.007 and 26,000 in./in./min are determined in this report.

FUNDAMENTAL STUDIES RELATING TO SYSTEMS ANALYSIS OF SOLID PROPELLANTS

Blatz, P. J., Knauss, W. G., et al
January 15, 1960
California Institute of Technology
Guggenheim Aeronautical Lab, Pasadena, Calif.
PR-5

This report presents a detailed examination of the properties of a filled viscoelastic resin and their representation by appropriate mechanical models. A comparison of two methods of computing viscoelastic strains in a pressurized cylinder is included.

QUARTERLY PROGRESS REPORT ON ENGINEERING RESEARCH

Parr, C. H. and Groetzinger, W. H., III
January 22, 1960
Rohm and Haas Co.
Redstone Arsenal Research Division, Huntsville, Ala., R-P-59-23

Equations expressing elastic stresses and strains in a three-material composite, hollow, circular cylinder representing a case-bonded propellant grain, liner, and motor case were derived for loading conditions consisting of internal pressure, arbitrary radial temperature gradient, and volumetric changes. The three materials were considered to be homogeneous and isotropic.

FRACTURE MECHANICS OF SOLID PROPELLANTS (U)

Jones, J. W., Sagers, D. L., et al
February 1960
DuPont de Nemours, E. I., & Co., Inc.
Explosives Dept., Wilmington, Del.
ELab-A-19 (Final Report) (CONFIDENTIAL)
NOrd-18138

Objectives for this program are to conduct investigations of the fracture mechanism of composite rocket propellants and to attempt to delineate relationships among fracture, temperature, propellant elasticity, distortion rate and propellant explosion susceptibility. This report summarizes the work accomplished in these investigations during the year ending February 15, 1960.

SOLID PROPELLANT AGING STUDIES

Beyer, R. B. and Fishman, N.
February 20, 1960
Stanford Research Institute, Menlo Park, Calif.
R 20, QR-7, November 1959–January 1960
(CONFIDENTIAL)

The open literature, as well as classified publications, has been searched for potential nondestructive evaluation techniques. A preliminary bibliography is presented.

REPORT ON NON-DESTRUCTIVE TEST METHODS USED ON POLARIS CHAMBERS AND CLOSURES

Cantor, B.
March 30, 1960
U.S. Naval Weapons Plant, Washington, D.C.
TM 115, NRL Project 62R19-05

References

1. Tenney, G. H., *A Study Report on the Present Status of Nondestructive Testing as Applied to Solid Propellants* (prepared for Advanced Research Projects Agency, Washington, D.C.), Los Alamos Scientific Laboratory, Los Alamos, New Mexico, October 15, 1958 (Confidential).

2. Tenney, G. H., *Nondestructive Techniques for the Determination of Physical Integrity of Rocket Motors*, pp 175–180, Solid Propellant Information Agency, Silver Spring, Maryland, August 1959 (Confidential).

3. Biatz, P. J., "Fracture Studies on Composite Solid Propellants," *Nondestructive Techniques for the Determination of Physical Integrity of Rocket Motors*, pp 145–156, Solid Propellant Information Agency, Silver Spring, Maryland, August 1959 (Confidential).

4. Allegretto, D. P., and Painter, B. D., "Photographic Studies of the Effect of Grain Defects on the Burning Characteristics of Highly Aluminized Composite Solid Propellants," *Bulletin of the 16th Meeting JANAF Solid Propellant Group*, Solid Propellant Information Agency, Silver Spring, Maryland, June 1960 (Confidential).

5. *Method of Determining the Tensile Properties of Solid Rocket Propellants. Part II. Composite Propellants.* Publication No. SP1A/PP8, Solid Propellant Information Agency, Silver Spring, Maryland, February 1957 (Confidential).

6. Smith, T. L. and Coy, J. L., "The Storage Stability of Some Ammonium Perchlorate-Polyurethane Propellants," *Bulletin of the Third Meeting, JANAF Solid Propellant Surveillance Panel*, Publication No. SPSP/5, The Solid Propellant Information Agency, Silver Spring, Maryland, October 1958 (Confidential), also Publication No. 138, Jet Propulsion Laboratory, Pasadena, California, August 29, 1958 (Confidential).

7. Hiester, N. K., *Aging Properties of Solid Propellants for Rocket Motors*, Technical Report No. I, Project C-938, Stanford Research Institute, Menlo Park, California, February 18, 1955.

8. Ryskiewicz, E. E. and Fishman, N., *Aging Properties of Solid Propellants for Rocket Motors*, Technical Report No. II, Project C-938, Stanford Research Institute, Menlo Park, California, October 19, 1955 (Confidential).

9. Fishman, N., *Aging Properties of Solid Propellants for Rocket Motors*, Technical Report No. I, Project No. C-1406, Stanford Research Institute, Menlo Park, California, May 21, 1956 (Confidential).

10. Fishman, N., *Aging Properties of Solid Propellants for Rocket Motors*, Technical Report No. II, Project No. C-1406, Stanford Research Institute, Menlo Park, California, February 4, 1957 (Confidential).

11. Fishman, N., *Aging Properties of Solid Propellants for Rocket Engines*, Technical Report No. III, Project No. C-1406, Stanford Research Institute, Menlo Park, California, July 15, 1957 (Confidential).

12. Davis, R. T., "Effects of Moisture on Storage Stability of Ammonium Perchlorate Propellants," *Bulletin of the Fourth Meeting, JANAF Solid Propellant Surveillance Panel*, Publication No. SPSP/7, The Solid Propellant Information Agency, Silver Spring, Maryland, November 1959.

13. *Combined Bimonthly Summary No. 57*, Jet Propulsion Laboratory, Pasadena, California, February 15, 1957 (Confidential).

14. *Combined Bimonthly Summary No. 67*, Jet Propulsion Laboratory, Pasadena, California, October 15, 1958 (Confidential).

15. *Research Summary No. 4*, Jet Propulsion Laboratory, Pasadena, California, August 15, 1959 (Confidential).

16. *Research Summary No. 36-3, Volume II*, Jet Propulsion Laboratory, Pasadena, California, July 1, 1960 (Confidential).

17. *Combined Bimonthly Summary No. 40*, Jet Propulsion Laboratory, Pasadena, California, March 20, 1954 (Confidential).

18. *Combined Bimonthly Summary No. 66*, Jet Propulsion Laboratory, Pasadena, California, p 11, August 15, 1958.

19. Smith, T. L., *Volume Changes and Dewetting in Glass Bead-Polyvinyl Chloride Elastomeric Composites Under Large Deformations*, Progress Report No. 30-2, Jet Propulsion Laboratory, Pasadena, California, January 2, 1959.